Journal of Quantitative Spectroscopy & Radiative Transfer 110 (2009) 1781–1800

Contents lists available at ScienceDirect

Journal of Quantitative Spectroscopy & Radiative Transfer

journal homepage: www.elsevier.com/locate/jqsrt

High sensitivity CW-CRDS of ^{18}O enriched water near 1.6 μm

Anwen Liu [a,b], Olga Naumenko [c], Samir Kassi [a], A. Campargue [a,*]

[a] Laboratoire de Spectrométrie Physique (associated with CNRS, UMR 5588), Université Joseph Fourier de Grenoble, B.P. 87, 38402 Saint-Martin-d'Hères Cedex, France

[b] Hefei National Laboratory for Physical Sciences at Microscale, Department of Chemical Physics, University of Science and Technology of China, Hefei 230026, China

[c] Institute of Atmospheric Optics, Russian Academy of Sciences, Siberian Branch, Tomsk 634055, Akademicheskii av.,1, Russia

ARTICLE INFO

Article history:
Received 6 March 2009
Received in revised form
17 April 2009
Accepted 20 April 2009

Keywords:
Cavity ring down spectroscopy
Water
$H_2{}^{18}O$
$H_2{}^{17}O$
H_2O
$HD^{18}O$
Rovibrational assignments
HITRAN
MARVEL

ABSTRACT

The absorption spectrum of ^{18}O enriched water has been recorded by continuous wave cavity ring down spectroscopy between 5905.7 and 6725.7 cm^{-1} using a series of fibred DFB lasers. The investigated spectral region corresponds to the important 1.55 μm transparency window of the atmosphere where water absorption is very weak. The typical CRDS sensitivity (noise equivalent absorption of 5×10^{-10} cm^{-1}) allowed for the detection of lines with intensity as low as 10^{-28} cm/molecule while the minimum intensity value provided by HITRAN in the considered spectral region is 1.7×10^{-24} cm/molecule. The line parameters were retrieved with the help of an interactive least squares multi-lines fitting program assuming a Voigt function as line profile. Overall, 4510 absorption lines belonging to the $H_2{}^{18}O$, $H_2{}^{16}O$, $HD^{18}O$, $HD^{16}O$ and $H_2{}^{17}O$ water isotopologues were measured. Their intensities range between 3×10^{-29} and 5×10^{-23} cm/molecule at 296 K and the typical accuracy on the line positions is 1×10^{-3} cm^{-1}. 2074 of the observed lines attributed to $H_2{}^{18}O$, $HD^{18}O$ and $H_2{}^{17}O$ are reported for the first time. The transitions were assigned on the basis of variational calculations resulting in 288, 135 and 38 newly determined rovibrational energy levels for the $H_2{}^{18}O$, $HD^{18}O$ and $H_2{}^{17}O$ isotopologues, respectively. The new data set includes the band origin of the $4\nu_2$ bending overtone of $H_2{}^{18}O$ at 6110.4239 cm^{-1} and rovibrational levels corresponding to J and K_a values up to 18 and 12, respectively, for the strongest bands of $H_2{}^{18}O$: $4\nu_2$, $\nu_1+2\nu_2$, $2\nu_2+\nu_3$, $2\nu_1$, $\nu_1+\nu_3$, and $\nu_2+\nu_3$. The obtained experimental results have been compared to the spectroscopic parameters provided by the HITRAN database and to the recent IUPAC critical review of the rovibrational spectrum of $H_2{}^{18}O$ and $H_2{}^{17}O$ as well as to variational calculations. Large discrepancies between the $4\nu_2$ variationally predicted and experimental intensities have been evidenced for the $H_2{}^{18}O$ and $H_2{}^{16}O$ molecules.

1. Introduction

In spite of its low relative concentration compared to the main isotopologue (3.1×10^{-3}), $H_2{}^{18}O$ is the fifth most important atmospheric absorber. Due to the vibrational isotopic shift, the relative contribution of the $H_2{}^{18}O$ absorption may largely exceed its relative abundance in some spectral regions. Such situations may occur in the regions corresponding to very weak absorption as the presently studied 1.55 μm transparency window. In the 6000–8000 cm^{-1} range including our

* Corresponding author. Tel.: +33 4 76 51 43 19; fax: +33 4 76 63 54 95.
E-mail address: Alain.Campargue@ujf-grenoble.fr (A. Campargue).

0022-4073/$ - see front matter © 2009 Elsevier Ltd. All rights reserved.
doi:10.1016/j.jqsrt.2009.04.013

region of interest, the HITRAN database in its last versions [1,2] provides for $H_2{}^{18}O$ the spectroscopic parameters obtained by Chevillard et al. [3] and Toth [4] by Fourier transform spectroscopy (FTS). These FTS spectra were recorded with ^{18}O enriched water in various experimental conditions. The maximum ^{18}O enrichment and pathlengths were (73%, 217.4 m) and (31.4%, 2.39 m) for the recordings of Refs. [3,4], respectively. The minimum intensity values provided in the HITRAN database in our region are on the order of 2×10^{-24} cm/molecule (for pure $H_2{}^{18}O$). Recently, the detection limit was lowered by nearly two orders of magnitude from FTS spectra recorded between 1000 and 8000 cm^{-1} at USTC (Hefei) with 95% ^{18}O enrichment and a 105 m absorption pathlength [5,6].

A still higher sensitivity can be achieved by continuous wave cavity ring down spectroscopy (CW-CRDS). Our preceding studies of water in natural isotopic abundance [7,8] have shown that transitions with intensity as low as 10^{-29} cm/molecule can be detected and measured.

The present work is devoted to a detailed analysis of the highly sensitive CW-CRDS ^{18}O enriched water spectrum between 1.69 and 1.49 μm (5905.7–6725.7 cm^{-1}).

After the description of the experimental set up and of the presentation of the retrieval of the spectroscopic parameters (Section 2), we will present the rovibrational analysis using the results of the variational calculations performed by Shirin et al. [9] and Schwenke and Partridge (SP) [10]. The SP line lists of the different water isotopologues can be downloaded from the http://spectra.iao.ru web site. The obtained results relative to the $H_2{}^{18}O$ and $H_2{}^{17}O$ isotopologues will be compared to the very recent exhaustive review of rovibrational line positions and levels of $H_2{}^{17}O$ and $H_2{}^{18}O$ [11] performed by an IUPAC sponsored task group (TG).

Under the project "A database of water transitions from experiment and theory", this IUPAC task group aims at an exhaustive evaluation of rovibrational line positions, transition intensities, energy levels and assignments for all the main isotopologues of water. By using the procedure and code MARVEL (Measured Active Rotational–Vibrational Energy Levels) [12,13], *all* the high quality experimental data available in the literature have been reviewed to determine and validate the $H_2{}^{18}O$ and $H_2{}^{17}O$ energy levels together with their self consistent uncertainties. The experimental $H_2{}^{18}O$ line positions used to derive the MARVEL energy levels in our region include studies based on spectra recorded with water in natural isotopic abundance—[14] (107 lines), [8] (61 lines) and [7] (386 lines)—or with ^{18}O enriched samples—[15] (35 lines), [16] (1 line), [3] (367 lines), [4] (60 lines), [5] (49 lines) and [6] (626 lines). It is worth noting that the high sensitivity achieved either by CW-CRDS [7,8] or by FTS with long absorption path lengths [14] allowed compensating the low $H_2{}^{18}O$ concentration in natural isotopic abundance and provided a significant amount of observations. Up to the present work, the Hefei spectra [5,6] provided the highest detectivity of $H_2{}^{18}O$ transitions in the region and then the largest amount of transitions used in the MARVEL procedure [11].

The $H_2{}^{18}O$ and $H_2{}^{17}O$ lines validated and recommended by the IUPAC TG have been deposited with their corresponding references as Supplementary Material of Ref. [11]. We will then refer to the 5905.7–6725.7 cm^{-1} section of these line lists for the comparison to our observations. Hereafter, we will called "IUPAC TG transitions and levels" the transitions and energy levels provided in Ref. [11].

The IUPAC TG transitions include a total of 1691 and 228 entries for the $H_2{}^{18}O$ and $H_2{}^{17}O$ species respectively. Taking into account that a given spectral line may have been measured in several experimental works, they correspond to 754 and 185 distinct transitions. As upper energy levels determined in the present study may have been accessed through transitions located in different spectral regions (this is in particular the case of the presently observed hot bands), we will also compare our energy levels values to the complete set of 4851 and 2687 energy levels validated by MARVEL code [11] for the $H_2{}^{18}O$ and $H_2{}^{17}O$ isotopologues, respectively.

2. Experiment and data reduction

2.1. The CW-CRDS spectrometer

We have developed a fibred CW-CRDS spectrometer using DFB diode lasers dedicated to the characterization of the important 1.5 μm atmospheric window of transparency. The typical achieved sensitivity of 2.5×10^{-10} cm^{-1} and the 4–5 decades dynamics on the intensity scale, have allowed to significantly improve the knowledge of the absorption spectrum of species of major atmospheric interest: H_2O [7,8], $^{12}CO_2$ [16,17], $^{13}CO_2$ [18], N_2O [19] and ozone [20]. This spectrometer was described in details in Refs. [7,21,22]. Briefly, 38 fibred DFB diode lasers were used to cover the 5905–6726 cm^{-1} region, each of them having a typical tuning range of 7 nm (~30 cm^{-1}) by temperature variation from −10 to 60 °C within about 70 min. The spectrum could be continuously covered except two gaps between 6122.3 and 6131.4 cm^{-1} and 6655.6 and 6667.1 cm^{-1}.

The ringdown cell temperature (typical value 299 K) and the gas pressure, measured by a capacitance gauge (MKS Baratron, 10 Torr range) were monitored during the spectrum acquisition. The spectrum in the 5905–6587 cm^{-1} region was recorded with 10 Torr. Lower pressures of about 0.1–1 Torr were used as lines with intensities as high as 10^{-23} cm/molecule are observed above 6587 cm^{-1}. An overview of the CW-CRDS spectrum is presented in Fig. 1. The small section presented in Fig. 2 illustrates the high signal to noise ratio of the spectra and that the noise equivalent absorption defined as the *rms* value of the noise level is about 5×10^{-10} cm^{-1}.

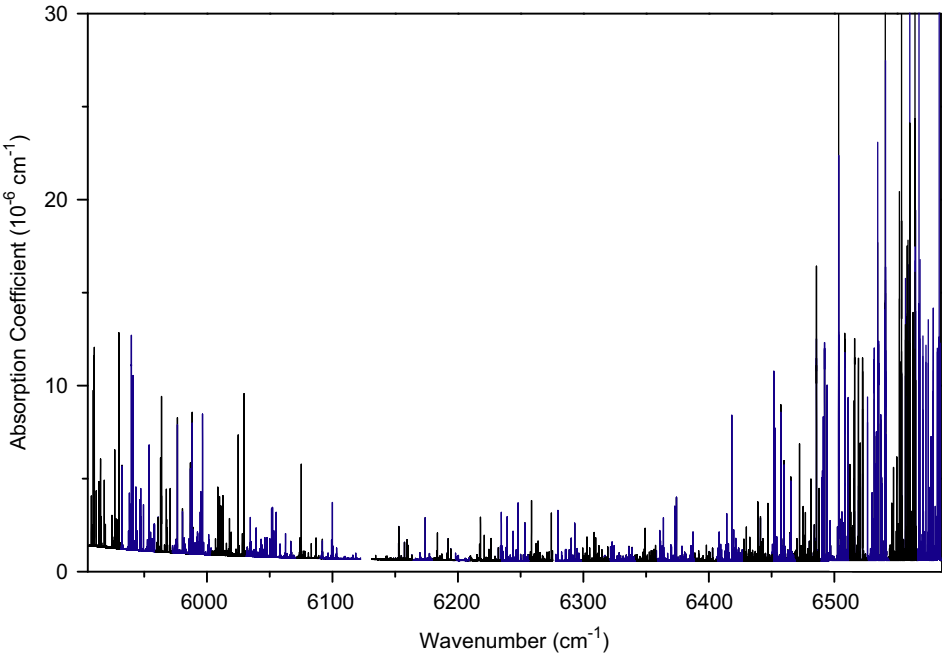

Fig. 1. Overview of the CW-CRDS spectrum of ^{18}O enriched water between 5905 and 6586 cm^{-1}. The sample pressure was about 10 Torr. The displayed spectrum was obtained by concatenating 30 individual spectra recorded successively with different DFB laser sources. The CW-CRDS spectrum is observed above the baseline fixed by the reflectivity of the used super mirrors.

2.2. Line parameter retrieval

The wavenumber calibration of the spectrum is based on the values provided by a wavemeter (Burleigh WA1640) and has been described in details in Ref. [22]. The wavenumber accuracy is checked and refined by using a few reference lines for each spectral section covered with one DFB laser. We adopted the FTS line positions of $H_2{}^{18}O$ from Refs. [5,6] as reference wavenumbers. As a result, reproducibility better than $2\times10^{-4}\,cm^{-1}$ could be achieved in the overlapping part of two successive spectral regions. Maximum deviations of $1.5\times10^{-3}\,cm^{-1}$ were observed for a few $H_2{}^{18}O$ reference lines which are then claimed as maximum uncertainty on the line positions.

The line parameters were obtained by using an interactive least squares multi-lines fitting program. As the DFB linewidth is much smaller than the Doppler broadening (1–5 MHz compared to 1 GHz), the contribution of the apparatus function to the observed profiles was neglected. A Voigt profile was adopted for each line. The width of the Gaussian component was fixed to the calculated Doppler broadening. Line position, integrated line absorbance, Lorentzian contributions of each line and a baseline (assumed to be a linear function of the wavenumber) were provided by the fitting procedure. Fig. 3 illustrates the achieved agreement in two spectral regions showing transitions with intensities differing by more than four orders of magnitude (the weakest lines on the left hand panel have an intensity of 6.0×10^{-28} cm/molecule while the strongest line on the right hand panel corresponds to a 8.2×10^{-24} cm/molecule intensity value). The calculated minus observed deviations show maximum values of several % for the strongest lines. This value is clearly higher than the noise level, indicating that a more sophisticated profile including narrowing effects would probably improve the simulation. Nevertheless, the uncertainty on the integrated absorption coefficient (which is proportional to the line intensity) is much smaller, probably on the order of 1% for the lines of medium intensities. An alternative explanation of the observed line profile of the strongest transitions (intensities larger than 10^{-24} cm/molecule) is that in the case of strong absorption, the ring down time decreases to a very small value and the accuracy of the intensity values may be affected by the insufficient band pass of the data acquisition card. From the comparison with the variationally predicted intensities (see below), it seems that the uncertainty on our intensity values is on the order of 5% for the few tens of transitions with intensities larger than 10^{-24} cm/molecule. In addition, the intensities of these strong lines were obtained from spectra recorded at lower pressure (less than 1 Torr) and the uncertainty on the intensity values may have been affected by larger errors on the pressure values.

As a result of the continuous exchange of water molecules in the gas phase and $H_2{}^{16}O$ molecules absorbed on the walls of the CRDS cell, the relative abundance of the $H_2{}^{18}O$ and $H_2{}^{16}O$ isotopologues may vary from one DFB laser scan to the next one. Instead of deriving directly the $H_2{}^{18}O$ concentration by using the line intensity values available

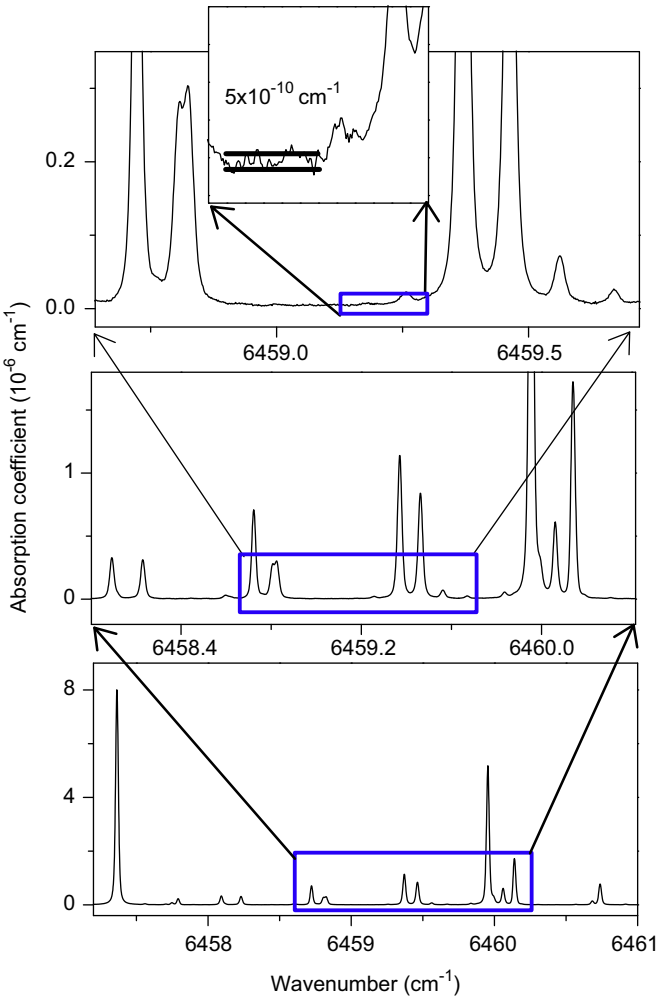

Fig. 2. Zoom of the CW-CRDS spectrum of water near 6459 cm^{-1} recorded at a pressure of 9.1 Torr. Three successive enlargements illustrate the achieved signal to noise ratio while the insert shows that the noise equivalent absorption (defined as the *rms* value of the noise level) is about 5×10^{-10} cm^{-1}.

for this isotopologue in our region, we calculated it as the difference of the total molecular concentration and the $H_2{}^{16}O$ concentration. This indirect method has the advantage of using line strengths values of the $H_2{}^{16}O$ main isotopologue which are believed to be more reliable than those available for the $H_2{}^{18}O$ species itself. An additional advantage is that, $H_2{}^{18}O$ being dominant in our sample, the resulting uncertainty on its relative concentration is expected to be lower. For each spectrum corresponding to one DFB laser scan, the $H_2{}^{16}O$ concentration was obtained as the average value of the concentration calculated from a number of well isolated $H_2{}^{16}O$ lines. For each selected $H_2{}^{16}O$ transition, the concentration value was obtained as the ratio of the integrated absorbance by the absolute line intensity provided by HITRAN [1]. The concentration of deuterated and ^{17}O isotopologues in the water sample being negligible compared to two main isotopologues ($H_2{}^{18}O$ and $H_2{}^{16}O$) (see below), the absolute concentration of the $H_2{}^{18}O$ isotopologue was then obtained by difference between the total molecular concentration deduced from the measured pressure value and the obtained $H_2{}^{16}O$ concentration. The obtained values of the $H_2{}^{18}O$ abundance range between 84.0% and 92.1% according to the recordings.

The absolute intensity of each $H_2{}^{18}O$ line was then calculated as the ratio of the integrated absorbance provided by the line profile fitting by the corresponding $H_2{}^{18}O$ molecular concentration.

The intensity criterion is of importance for the assignment of the spectrum. In order to assign the transitions of the minor isotopologues ($HD^{18}O$, $H_2{}^{17}O$ and $HD^{16}O$), an estimation of their relative abundance is then necessary. By comparison with variationally calculated intensities [9,10,24], we obtained the following average abundances: $H_2{}^{17}O$: 3.0×10^{-3}, $HD^{16}O$: 3.8×10^{-5} and $HD^{18}O$: 2.8×10^{-4}, while the $H_2{}^{16}O$ value was fixed to 10%. Note that these values are relative to pure $H_2{}^{18}O$ and not to the total molecular concentration.

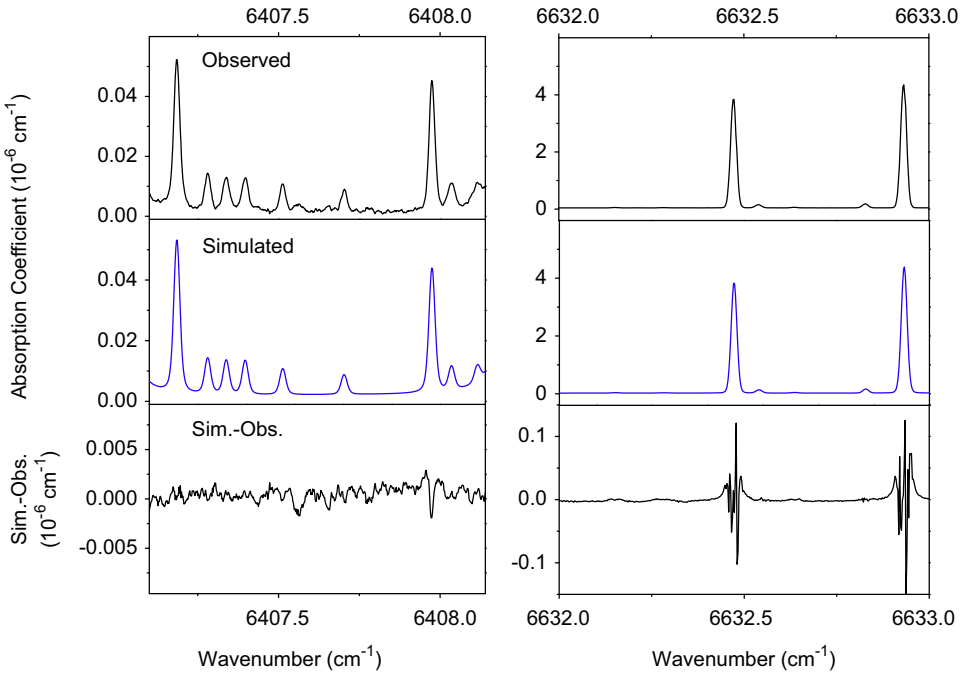

Fig. 3. Comparison of the CW-CRDS spectrum of water with a simulated spectrum obtained as a sum of individual Voigt profiles. The weakest lines of the left hand panel are about four orders of magnitude weaker than the two lines dominating the right hand spectrum. The residuals are displayed on the lower panel with a magnification factor. Experimental conditions: $T = 299$ K, $P = 13.2$ hPa (right panel) and $P = 13.6$ hPa (left panel).

3. Assignments and comparison with databases

3.1. Spectrum assignment and energy levels derivation and validation

Overall, 5320 lines were detected in the whole spectral region extending from 5905.7 to 6725.7 cm^{-1}. The detection of weak lines due to impurities present in the CRDS cell is a consequence of the achieved sensitivity. The most unexpected species that we could identify in the spectrum is the main isotopologue of carbonyl sulfide ($^{16}O^{12}C^{32}S$) which shows up by the $3\nu_3$ band near 6120 cm^{-1}. After removal of the transitions due to CO_2, C_2H_2, N_2O, CH_4, NH_3, and OCS, a list of 4732 transitions was obtained. The relative concentration of the impurities was estimated and found negligible (less than 0.2%) compared to water concentration.

By comparison with the FTS line lists of Refs. [7,8,14] and transitions set computed from the known experimental energy levels [11], 1072, 157 and 440 lines were easily assigned to the $H_2{}^{16}O$, $H_2{}^{17}O$ and $HD^{16}O$ isotopologues, respectively.

Obviously, most of the new experimental information concerns the $H_2{}^{18}O$ and $HD^{18}O$ species. The first step consisted in assigning new $H_2{}^{18}O$ transitions reaching known energy levels validated by MARVEL code [11]. The remaining transitions were assigned on the basis of variational calculations [9,10,23,24]. At the final stage, 39 weak new $H_2{}^{17}O$ lines were assigned leaving about 4% of the observed lines unassigned.

The final list consists in 4990 transitions assigned to five water isotopologues and corresponding to 4512 observed lines. This list is attached as Supplementary Material and provides for each line, the measured position, the rovibrational assignment and the variational intensity [9] scaled in accordance with the above isotopic composition of the sample. In addition, the measured intensity values are given for the $H_2{}^{18}O$ and $HD^{18}O$ isotopologues.

3.2. The $H_2{}^{18}O$ isotopologue

A total of 2015 transitions were assigned to this isotopologue. Taking into account a number of blended lines, they correspond to 1849 absorption lines. 1259 of them are reported for the first time. The overview comparison of the CW-CRDS spectrum with the $H_2{}^{18}O$ line lists provided by HITRAN or validated by the IUPAC TG is presented in Fig. 4. Overall, the number of $H_2{}^{18}O$ transitions has been multiplied by about 15 and 3 compared to the HITRAN [1,2] and IUPAC TG line lists, respectively. As illustrated by the overview spectra of Fig. 4, the CRDS detection limit (about 10^{-28} cm/molecule) lowers by more than four and two orders of magnitude those of the HITRAN (1.9×10^{-24} cm/molecule) and IUPAC TG lists (3.7×10^{-26} cm/molecule), respectively.

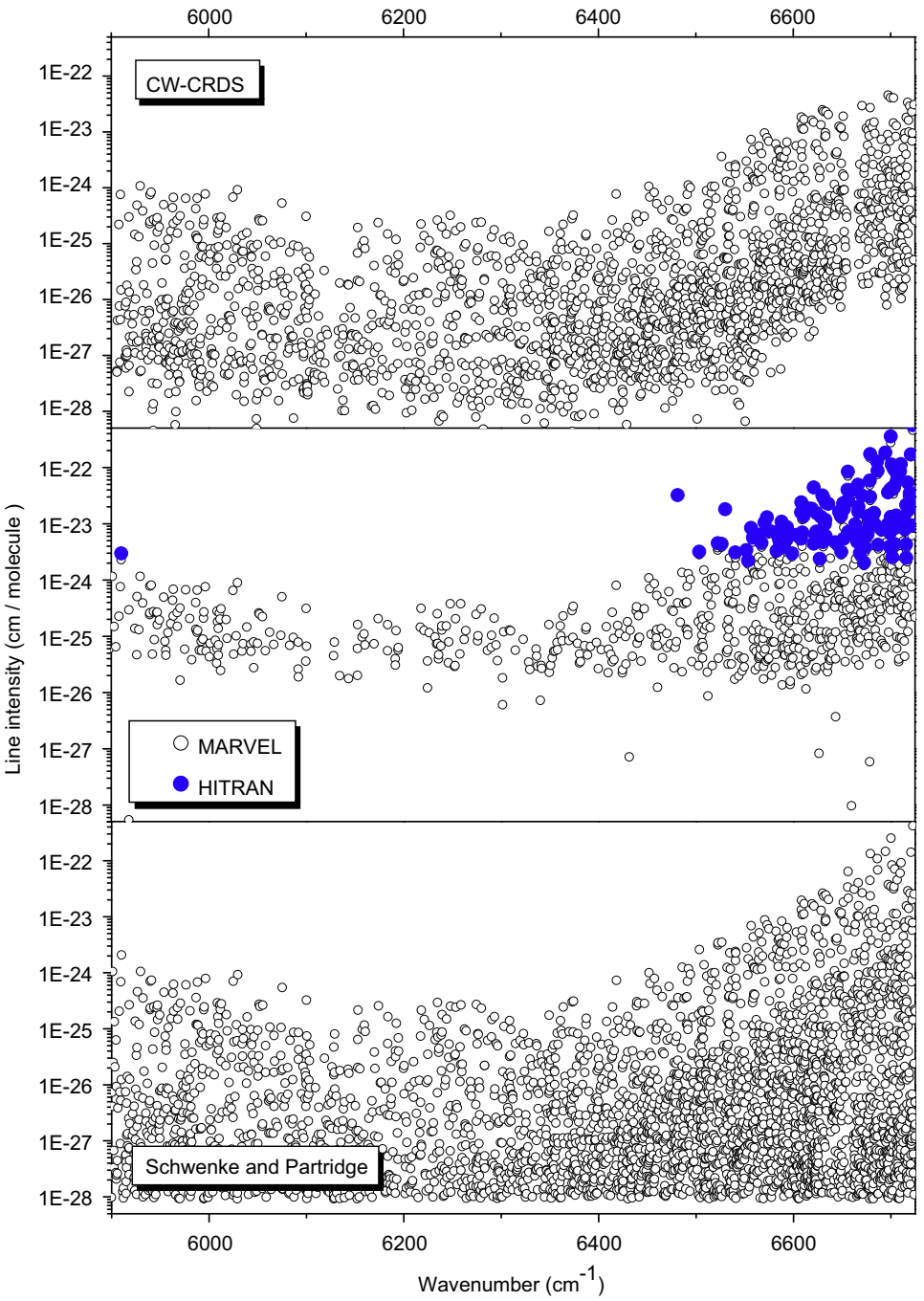

Fig. 4. Comparison of different line lists for the $H_2{}^{18}O$ absorption spectrum between 5905 and 6725 cm^{-1}. Note the logarithmic scale adopted for the line intensities. *Upper panel*: CW-CRDS. *Middle panel*: full circles: HITRAN database [1], open circles: IUPAC TG line list [11] mostly due to the FTS measurements of Refs. [5,6]. *Lower panel*: SP variational calculations [10].

The considered spectrum is mainly dominated by five cold bands of the first hexade of interacting vibrational states ($4\nu_2$, $\nu_1+2\nu_2$, $2\nu_2+\nu_3$, $2\nu_1$ and $\nu_1+\nu_3$) and two hot bands ($\nu_1+3\nu_2-\nu_2$ and $3\nu_2+\nu_3-\nu_2$). Fig. 5 shows an example of line assignments around 6312.5 cm^{-1}. The band by band comparison with HITRAN and IUPAC TG line lists is included in Table 1. Overall, transitions belonging to eighteen bands including nine hot bands were observed. The vibrational energy of the upper states as obtained by the MARVEL procedure [11] is provided in Table 1. It is interesting to underline that rotational levels of vibrational states with band origin located much below and much above the 5900–6700 cm^{-1} investigated region

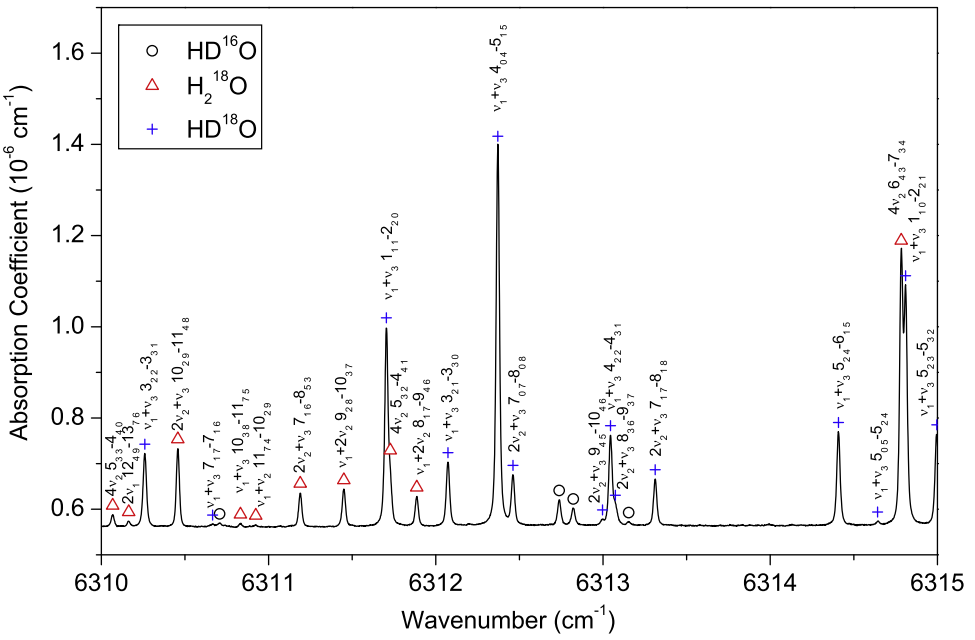

Fig. 5. Example of line assignments of the CW-CRDS spectrum of ^{18}O enriched water near 6313 cm^{-1}. Lines due to the $H_2{}^{18}O$, $HD^{18}O$ and $HD^{16}O$ isotopologues are indicated. The baseline fixed by the mirror losses was not substracted.

could be determined: energy levels of the (030) bending state at 4648.48 cm^{-1} were derived while transitions reaching the (041) vibrational state at 9795.33 cm^{-1} were detected through the $4\nu_2+\nu_3-2\nu_2$ hot band.

A total of 1128 $H_2{}^{18}O$ levels were obtained by adding to the measured wavenumber the energy value of the lower level [26]. For comparison, a total of 4851 $H_2{}^{18}O$ energy levels were derived by the MARVEL code from the exhaustive review of the literature [11]. The complete energy level list is provided as Supplementary material and includes the deviations of the observed levels from their variational values obtained by Shirin et al. [9]. Detailed comparison with IUPAC TG database, also included into the Supplementary material, yielded 288 new energy levels, which are presented in Table 2. They belong to eleven upper vibrational states, though most of them concern the (040), (011) and (120) states (see Table 1). Note that very weak transitions reaching levels with J and K_a values as large as 18 and 12 were detected for the strong $\nu_2+\nu_3$ band. The newly determined energy levels include 79 levels of the (040) state—in particular the origin of the $4\nu_2$ band at 6110.4238 cm^{-1}—and 24 energy levels of the (050) bending state for which only four energy levels were previously determined [11].

The energy values of the 838 levels in common with the IUPAC TG set show a good agreement with an *rms* deviation of 0.0020 cm^{-1}, excluding seven clear outliers (absolute discrepancies ranging between 0.012 and 0.036 cm^{-1}) which are marked in Table 2. All these outliers were reported as less reliable (C, B^-, and B+ types) in the classification of Ref. [11]. Six of them are newly derived from well resolved lines or are reliably supported by accurate combination differences relations.

As our assignments were based on variational calculations [9,10,23], and yielded energy levels with high J and K_a values, it is interesting to test the quality of the variational predictions in particular for high J and K_a values. The (obs.-calc.) differences of the energy levels are plotted versus $J+K_a|J$ in Fig. 6 both for SP [10,23] and Shirin et al. [9] databases. A pronounced J and K_a dependence is noted for Shirin et al. energy values: the deviations are small (and generally negative) for small K_a values, then decrease down to a negative minimum at about $K_a = J/2$ and sharply increase up to a large positive values for K_a values approaching J. The corresponding *rms* deviation is 0.05 cm^{-1}, with maximum difference of +0.29 cm^{-1}. These values largely exceed the claimed "experimental" accuracy of the calculations of Ref. [9]. The deviations of SP predictions from the observed levels do not show a clear K_a dependence, they are mostly positive with *rms* deviation and maximum amplitude of 0.07 and 0.38 cm^{-1}, respectively. Note that for J values higher than 12, some SP predictions start to deviate importantly.

3.3. The $HD^{18}O$ isotopologue

In spite of a low relative concentration compared to the $H_2{}^{18}O$ species (about 2.8×10^{-4} in our sample), transitions of the $HD^{18}O$ isotopologue show up with similar absorbance than those of the $H_2{}^{18}O$ species. This is due to the considerable shift of the vibrational band centres induced by the H/D isotopic substitution. The situation is very similar for the

Table 1
Comparison of the amount of $H_2{}^{18}O$, $H_2{}^{17}O$, $HD^{18}O$ transitions observed by CW-CRDS in the 5905.7–6725.7 cm^{-1} region with those provided by the HITRAN, IUPAC [11] and Ref. [25] databases in the same region.

Band	Upper state energy (cm^{-1})[a]	Number of transitions			Levels[b]	
		CW-CRDS	HITRAN	IUPAC TG [11]	Total	New
$H_2^{18}O$						
(030)–(000)	4648.4778	19			19	
(110)–(000)	5221.2433	73			58	24
(011)–(000)	5310.4613	176	1	53	130	40
(040)–(000)	[6110.43] 6110.4238	471	2	159	156	79
(120)–(000)	6755.5102	320	63	197	163	41
(021)–(000)/(021)–(010)	6844.5987	324/14	53	196/1	152	25
(200)–(000)/(200)–(010)	7185.8781	119/3	5	48/1	107	26
(101)–(000)/(101)–(010)	7228.8833	131/3	1	46	98	2
(002)–(000)/(002)–(010)	7418.7241	32/53	1	6	72	4
(050)–(010)	[7514.21]	33			26	24
(130)–(010)	8249.0357	102		6	62	3
(031)–(010)	8341.1079	139		42	82	4
(111)–(010)	8779.7195	1			1	
(041)–(020)	9795.3315	2			2	
Total		**2015**	**126**	**754**	**1128**	**288**
$H_2^{17}O$						
(011)–(000)	5320.2512	31		6	31	12
(040)–(000)	[6121.55]	44		23	31	16
(120)–(000)	6764.7256	76		73	60	10
(021)–(000)	6857.2726	58		74	48	
(200)–(000)	7193.2464	2		4	1	
(101)–(000)	7238.7140	1		3	1	
Total		**212**		**183**	**172**	**38**
$HD^{18}O$						
		CW-CRDS		Ref. [25]		
(101)–(000)	6390.9831	674		199	135	60
(021)–(000)	6425.9515	332		101	106	45
(050)–(000)	[6659.39]	4			4	4
(210)–(000)	6711.6726	89		31	62	26
Total		**1099**		**331**	**307**	**135**

[a] Vibrational band origins as obtained by the MARVEL procedure as part of the IUPAC TG effort [11] for $H_2{}^{18}O$ and $H_2{}^{17}O$, or derived in this study for $HD^{18}O$. In absence of experimental values, the variational estimations from Ref. [9] for $H_2{}^{18}O$ and $H_2{}^{17}O$, and from Ref. [24] for $HD^{18}O$ are provided in brackets. The energy value of the (040) is newly determined from the present work. The band origin is identical to the upper energy level for the cold bands and can be obtained by subtracting 1588.2759, and 3139.0500 cm^{-1} for the hot bands originating from the (010), and (020) lower state, respectively.

[b] Number of upper energy levels determined from the CW-CRDS analysis and number of new determinations compared to the lists of Refs. [11,25].

absorption spectrum of water in natural abundance: the $HD^{16}O$ absorbance in the same transparency window was found to represent one third of the $H_2{}^{16}O$ absorbance [7].

On the basis of SP calculations [10,24], 1099 transitions corresponding to 955 absorption lines were assigned to four bands of the $HD^{18}O$ isotopologue: $2\nu_2+\nu_3$, $\nu_1+\nu_3$, $2\nu_1+\nu_2$, and $5\nu_2$ (see the statistics included in Table 1). It led to the derivation of 307 levels which are provided as Supplementary Material. At the final stage of our identification of the $HD^{18}O$ transitions, we became aware of the results of Ref. [25] where $HD^{18}O$ transitions were newly assigned by FTS in the 4200–11 600 cm^{-1} region. These observations have been combined with all available literature sources to construct and validate a complete database for this isotopologue. The validated transitions have been used to derive a set of 1699 consistent energy levels using the Rydberg–Ritz combination principle [25].

The complete comparison of our energy levels set with that of Ref. [25] is also included in the Supplementary material. The corresponding *rms* deviation is 0.0021 cm^{-1} after exclusion of nine outliers with disagreement between −0.025 and 0.012 cm^{-1} and two incorrect levels ([331] and [330] of the (210) state) with a deviation of about 0.055 cm^{-1}. In addition to the 172 levels in common with Ref. [25], 135 energy levels were determined. Table 3 lists these new levels with their corresponding (obs.-calc.) values. We have also included in this table our energy values of nine levels that we believe significantly more accurate than those of Ref. [25].

3.4. The $H_2{}^{17}O$ isotopologue

The ratio of the $H_2{}^{17}O$ and $H_2{}^{18}O$ concentrations in our sample was estimated to be 3.1×10^{-3}. After identification of the transitions of the other water isotopologues and the "trivial" assignments of 157 $H_2{}^{17}O$ transitions based on IUPAC TG

Table 2
New experimental energy levels of the $H_2{}^{18}O$ molecule (in cm^{-1}) derived by CW-CRDS in the 5905.7–6725.7 cm^{-1} region.

$V_1V_2V_3$	J	K_a	K_c	E_{obs}	δE	N	Δ	$V_1V_2V_3$	J	K_a	K_c	E_{obs}	δE	N	Δ
002	9	1	9	8305.5475		1	−0.02	021	16	1	15	9776.1745		1	−0.06
002	10	1	10	8493.0042		1	−0.03	021	17	0	17	9729.3843**		1	0.03
002	11	7	4	9624.0629		1	0.10	021	17	1	17	9729.3843**		1	0.03
002	14	1	14	9418.6869		1	−0.06	031	9	2	7	9597.3411		1	−0.01
011	11	10	2	8333.1681		1	0.18	031	9	3	6	9694.9965		1	−0.08
011	11	10	1	8333.1686		1	0.18	031	12	1	12	9853.9182		1	−0.03
011	11	11	1	8579.0583		1	0.24	031	12	2	11	10147.6537		1	−0.07
011	11	11	0	8579.0580		1	0.24	040	0	0	0	6110.4239		1	−0.01
011	12	8	5	8160.3503***		1	0.06	040	6	5	1	7404.5834	0.7	3	0.03
011	12	11	2	8873.6920		1	0.22	040	6	6	0	7680.6794*		1	0.06
011	12	11	1	8873.6920		1	0.22	040	7	5	3	7575.1607	0.5	3	0.02
011	12	12	1	9128.3760		1	0.29	040	7	7	1	8147.4666		1	0.10
011	12	12	0	9128.3760		1	0.29	040	7	7	0	8147.4668		1	0.10
011	13	7	6	8263.6746*		1	0.00	040	8	1	7	7061.5403	0.2	3	−0.04
011	13	8	5	8471.7182	0.7	2	0.04	040	8	2	6	7185.1330	0.2	4	−0.05
011	13	9	5	8698.4851		1	0.08	040	8	3	5	7318.7885	0.4	4	−0.04
011	13	9	4	8698.4885		1	0.08	040	8	4	4	7520.6398	0.3	4	−0.02
011	13	10	4	8939.2984		1	0.13	040	8	5	3	7770.0406	0.6	2	0.01
011	13	10	3	8939.2956		1	0.13	040	8	6	3	8048.3736	0.5	2	0.05
011	14	7	8	8596.4041		1	−0.03	040	8	6	2	8048.3808		1	0.04
011	14	8	7	8805.2858		1	0.01	040	8	7	1	8344.3675		1	0.09
011	14	8	6	8805.4860	0.5	2	0.01	040	8	8	1	8650.4343		1	0.15
011	14	9	5	9032.9075		1	0.06	040	8	8	0	8650.4321		1	0.15
011	14	10	5	9275.3240		1	0.11	040	9	2	8	7293.2265	0.3	4	−0.03
011	14	10	4	9275.3276		1	0.11	040	9	2	7	7416.5484	0.3	4	−0.06
011	14	11	3	9528.8244		1	0.17	040	9	3	7	7511.3628	0.4	3	−0.04
011	15	5	10	8688.9199		1	−0.02	040	9	3	6	7547.8225	0.3	4	−0.06
011	15	6	9	8792.0731	0.4	2	−0.10	040	9	4	6	7736.0379	0.1	4	−0.02
011	15	7	9	8952.1455		1	−0.04	040	9	5	5	7986.4636	0.1	2	0.00
011	15	7	8	8957.2058	1.9	2	−0.06	040	9	5	4	7988.4993		1	0.00
011	15	8	8	9160.9542		1	−0.01	040	9	6	3	8267.8383		1	0.04
011	15	8	7	9161.4860		1	−0.01	040	9	7	3	8564.7838		1	0.08
011	15	9	7	9389.0405		1	0.04	040	9	8	2	8871.9306		1	0.13
011	15	9	6	9389.0784		1	0.03	040	9	8	1	8871.9309		1	0.13
011	16	3	13	8732.9500*		1	−0.04	040	9	9	1	9176.3241		1	0.19
011	16	4	13	8735.5591		1	−0.04	040	9	9	0	9176.3241		1	0.19
011	16	4	12	8929.3629		1	−0.06	040	10	0	10	7224.8553		1	−0.02
011	16	5	12	8945.5360		1	−0.07	040	10	1	9	7496.7810	0.2	3	−0.05
011	16	5	11	9075.2014		1	−0.05	040	10	2	9	7512.0383	0.1	3	−0.04
011	16	6	11	9136.6177		1	−0.09	040	10	2	8	7669.3031	0.3	3	−0.07
011	16	6	10	9184.6812		1	−0.14	040	10	3	7	7803.5485	0.9	2	−0.07
011	16	7	9	9339.6831		1	−0.13	040	10	4	7	7976.3337	0.6	4	−0.03
011	17	2	15	8843.6041		1	−0.02	040	10	4	6	7986.3577		1	−0.04
011	17	3	15	8843.0006		1	−0.02	040	10	5	5	8230.5896	1.4	2	−0.01
011	17	3	14	9101.3466**		1	0.03	040	10	6	5	8510.5472	0.8	2	0.03
011	17	4	14	9103.1863		1	−0.05	040	10	6	4	8510.7378		1	0.02
011	18	2	16	9210.3882		1	−0.03	040	10	7	4	8808.3885		1	0.07
021	11	7	4	9325.8026		1	0.05	040	10	7	3	8808.3876		1	0.07
021	11	8	4	9553.4410		1	0.11	040	10	8	3	9116.5033		1	0.12
021	11	8	3	9553.4410		1	0.11	040	10	8	2	9116.5033		1	0.12
021	12	5	8	9208.2545		1	−0.05	040	11	0	11	7433.0245	1.3	2	−0.01
021	12	7	5	9613.8517		1	0.02	040	11	1	11	7433.8104		1	−0.01
021	13	2	11	9121.2487		1	−0.06	040	11	1	10	7739.4371	0.6	2	−0.05
021	13	4	10	9328.5593	0.1	2	−0.07	040	11	2	10	7749.5948	0.2	2	−0.04
021	13	5	9	9516.7933		1	−0.06	040	11	2	9	7941.2979	0.2	2	−0.08
021	14	1	14	8852.4951		1	−0.04	040	11	3	9	8000.4988	0.8	2	−0.04
021	14	1	13	9167.5800		1	−0.05	040	11	3	8	8084.6403		1	−0.08
021	14	2	13	9164.0245		1	−0.04	040	11	4	8	8238.2082	0.9	2	−0.04
021	14	3	12	9424.6407		1	−0.06	040	11	4	7	8257.5962		1	−0.05
021	14	3	11	9631.5956		1	−0.09	040	11	5	6	8496.2166		1	−0.02
021	14	4	10	9783.3508		1	−0.09	040	12	0	12	7658.6298		1	−0.01
021	14	5	9	9899.6472		1	−0.07	040	12	1	11	7998.9208		1	−0.05
021	15	0	15	9129.1192		1	0.02	040	12	2	11	8005.6176	0.6	3	−0.04
021	15	1	15	9129.0542	0.5	2	0.02	040	12	2	10	8229.7413		1	−0.08
021	15	2	14	9462.7478		1	−0.04	040	12	3	9	8389.2484		1	−0.10
021	15	2	13	9740.2032		1	−0.04	040	12	4	9	8515.1383	1.5	2	−0.03
021	15	4	12	9983.4275		1	−0.07	040	12	4	8	8554.7442		1	−0.07
021	16	0	16	9420.7128	1.1	2	0.02	040	12	5	7	8785.3557		1	−0.04
021	16	1	16	9420.6942		1	0.02	040	12	6	7	9064.8606		1	0.00

Table 2 (*continued*)

$V_1V_2V_3$	J	K_a	K_c	E_{obs}	δE	N	Δ	$V_1V_2V_3$	J	K_a	K_c	E_{obs}	δE	N	Δ
040	12	8	5	9673.3514		1	0.09	120	9	6	3	8542.9547		1	0.03
040	13	0	13	7901.7455		1	−0.01	120	9	8	2	9014.4883		1	0.10
040	13	1	13	7902.1157		1	−0.01	120	9	8	1	9014.4886		1	0.10
040	13	1	12	8275.5303		1	−0.05	120	10	6	5	8782.7722		1	0.02
040	13	2	12	8279.9952		1	−0.04	120	10	6	4	8783.1341		1	0.01
040	13	2	11	8539.6094		1	−0.07	120	10	8	3	9256.2287		1	0.09
040	13	3	10	8714.9109		1	−0.11	120	10	8	2	9256.2287		1	0.09
040	13	5	8	9098.0624		1	−0.04	120	10	9	2	9420.8426		1	0.18
040	14	0	14	8162.4660		1	−0.01	120	10	9	1	9420.8426		1	0.18
040	14	1	14	8162.7007		1	−0.03	120	11	1	11	8042.6492*	0.7	2	0.01
040	14	2	13	8572.4618		1	−0.04	120	11	4	8	8661.9199		1	−0.05
040	14	2	12	8862.8231		1	−0.07	120	11	5	7	8844.4388		1	−0.01
040	14	3	12	8884.1694		1	−0.06	120	11	5	6	8850.5369		1	−0.02
040	14	4	11	9155.3368		1	−0.05	120	11	6	6	9045.8852		1	0.00
040	14	5	10	9430.9214		1	−0.06	120	11	6	5	9046.0849		1	−0.01
040	15	0	15	8440.9141		1	−0.01	120	11	8	4	9520.6916		1	0.10
040	15	1	15	8441.0531		1	−0.01	120	11	8	3	9520.6867		1	0.09
040	16	1	16	8737.2342		1	0.05	120	12	1	11	8527.9848	0.1	2	−0.01
050	2	1	2	7633.8790		1	0.00	120	12	2	11	8537.9506	0.5	2	−0.03
050	3	2	1	7870.0850	1.2	2	0.01	120	12	2	10	8742.8155		1	−0.04
050	3	3	0	8085.8851		1	0.04	120	12	4	8	9005.5285		1	−0.06
050	4	1	4	7775.4735		1	0.00	120	12	5	7	9142.5996		1	−0.04
050	4	2	3	7962.1450	0.1	2	0.01	120	12	6	7	9331.8932		1	0.00
050	4	2	2	7969.7429		1	0.01	120	12	6	6	9335.3608		1	−0.03
050	4	3	2	8182.7291	0.6	2	0.03	120	13	1	13	8500.4276	0.1	2	0.01
050	5	1	5	7875.3537		1	−0.01	120	13	1	12	8791.7550		1	−0.02
050	5	1	4	7969.7760		1	−0.02	120	13	2	12	8786.6338		1	−0.02
050	5	2	3	8096.2649		1	−0.01	120	13	2	11	9029.2298		1	−0.04
050	5	3	3	8303.6845		1	0.02	120	13	3	11	9028.7607		1	−0.04
050	5	3	2	8304.6184		1	0.02	120	13	4	9	9327.0439		1	−0.06
050	6	0	6	7974.7236		1	−0.02	120	13	5	8	9460.4091		1	−0.05
050	6	1	6	7994.0847		1	−0.01	120	14	0	14	8756.5782	1.1	2	0.01
050	6	1	5	8124.0865		1	−0.01	120	14	1	14	8756.7504	0.4	2	0.01
050	6	2	5	8219.1607		1	−0.01	120	14	2	13	9067.7948		1	−0.02
050	6	3	4	8448.4774		1	0.02	120	14	2	12	9332.2394		1	−0.05
050	7	0	7	8117.1778		1	−0.03	120	14	4	11	9555.4730		1	−0.07
050	7	1	7	8131.3151		1	−0.01	120	15	0	15	9029.9285		1	0.06
050	8	1	8	8286.7712		1	−0.01	120	15	1	15	9029.9935		1	0.06
050	8	2	7	8562.5965		1	0.00	120	15	1	14	9363.4614		1	−0.03
050	8	5	4	9376.2526	4.8	2	0.04	120	16	0	16	9320.2332		1	0.06
050	9	1	9	8460.2740		1	−0.02	120	16	1	16	9320.2757		1	0.07
050	10	1	10	8651.7352		1	−0.02	130	9	2	8	9367.7595		1	−0.06
101	12	7	5	9704.7880		1	−0.08	130	10	2	9	9581.3863		1	−0.05
101	14	2	13	9464.4251		1	−0.07	130	11	0	11	9535.9645		1	−0.03
110	9	9	0	7552.4550		1	0.05	200	10	9	2	9502.5085		1	0.15
110	10	9	2	7796.9497		1	0.05	200	10	9	1	9502.5085		1	0.15
110	10	9	1	7796.9493		1	0.05	200	11	7	5	9399.2921		1	−0.03
110	11	8	4	7819.9222		1	0.03	200	11	8	4	9589.6103		1	0.03
110	11	9	2	8064.5135		1	0.04	200	11	8	3	9589.6054		1	0.02
110	12	6	7	7688.7221		1	0.00	200	11	9	3	9765.7508		1	0.13
110	12	8	5	8107.5697		1	0.02	200	11	9	2	9765.7508		1	0.13
110	13	6	8	7998.4905		1	0.00	200	11	10	2	9958.2454		1	0.23
110	13	6	7	8003.8214	0.9	2	−0.02	200	11	10	1	9958.2454		1	0.23
110	13	7	6	8195.7678		1	0.00	200	11	11	1	10193.0928		1	0.29
110	14	2	12	7752.4565		1	−0.03	200	11	11	0	10193.0928		1	0.29
110	14	3	12	7750.6086		1	−0.02	200	12	7	6	9682.3445		1	−0.02
110	14	3	11	7951.4746		1	−0.03	200	12	7	5	9683.2799		1	−0.01
110	14	4	11	7958.5480		1	−0.04	200	12	8	5	9874.0393		1	0.04
110	14	6	9	8331.2503	0.3	2	−0.01	200	12	8	4	9874.0899		1	0.06
110	15	3	12	8289.2050		1	−0.06	200	13	3	11	9341.5903		1	−0.10
110	15	4	12	8291.1486		1	−0.04	200	13	4	10	9512.7860*		1	−0.11
110	15	4	11	8462.5565		1	−0.08	200	13	4	9	9625.7177		1	−0.09
110	15	5	11	8489.0887		1	−0.06	200	13	5	8	9717.8594		1	−0.14
110	15	6	10	8665.2369		1	−0.13	200	13	6	7	9830.0527		1	−0.09
110	16	4	13	8640.8868		1	−0.03	200	13	7	7	9988.0148		1	0.00
110	16	5	12	8853.4508		1	−0.05	200	13	7	6	9990.9555		1	0.00
110	16	6	11	9045.7775		1	−0.11	200	14	1	13	9417.1071		1	−0.10
110	17	2	15	8746.7761		1	−0.01	200	14	2	13	9417.1526		1	−0.10
120	7	6	2	8133.4857*		1	0.04	200	14	3	12	9632.4921		1	−0.12
120	7	6	1	8133.4851*		1	0.04	200	14	6	9	10151.0559		1	−0.06

Table 2 (*continued*)

$V_1V_2V_3$	J	K_a	K_c	E_{obs}	δE	N	Δ	$V_1V_2V_3$	J	K_a	K_c	E_{obs}	δE	N	Δ
120	9	6	4	8542.8491		1	0.02	200	15	1	14	9707.8865		1	−0.07
030	9	8	2	7162.5060		1	0.11	030	11	9	2	7963.3613		1	0.13
030	9	9	1	7448.4693		1	0.15	030	12	8	4	7966.1994		1	0.08
030	9	9	0	7448.4691		1	0.15	030	12	10	3	8633.0787		1	0.10
030	10	8	3	7407.5575		1	0.09	030	12	10	2	8633.0787		1	0.10
030	10	8	2	7407.5568		1	0.09	030	14	5	10	7821.9787		1	−0.04
030	10	9	2	7694.5331		1	0.14	030	14	6	9	8066.9898		1	−0.03
030	11	8	4	7675.5709		1	0.09	030	15	4	11	8052.7787		1	−0.10
030	11	8	3	7675.5705		1	0.09	030	15	5	11	8176.4103		1	0.01

Notes: N is the number of lines used for the upper level determination. δE (in 10^{-3} cm^{-1}) denotes the corresponding statistical error defined as the *rms* value of the deviation of the levels derived through several transitions. Δ represents the deviation of the experimental level from its calculated [9] value in cm^{-1}. The energies of the levels marked by * were previously derived [11] with a different value (absolute deviations between 0.011 and 0.036 cm^{-1}). The three levels marked by ** have been obtained using calculated lower levels and their values can be less accurate. The [12 8 5] (011) level marked by *** was previously derived in Ref. [5] but not included in [11].

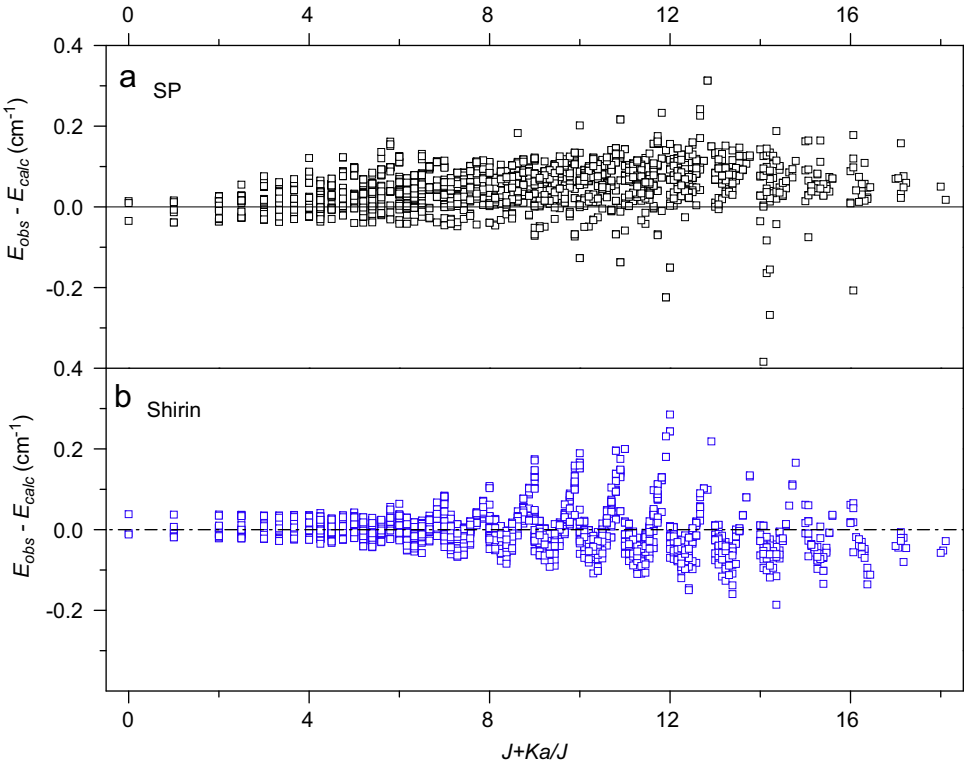

Fig. 6. Difference between the experimental and variationally computed energy values of the 1128 energy levels of $H_2{}^{18}O$ derived by CW-CRDS between 5905 and 6725 cm^{-1}, versus the quantity $J+K_a/J$. *Upper panel*: calculated values were obtained by Schwenke and Partridge [23]. *Lower panel*: calculated values were obtained by Shirin et al. [9].

energy levels, 39 very weak new $H_2{}^{17}O$ absorption lines were assigned. These newly assigned transitions allowed deriving 38 new energy levels (see Tables 1 and 4) belonging to the following vibrational states: (011) (12 levels), (040) (16 levels), and (120) (10 levels). Two IUPAC TG levels, [881] and [880] of the (011) state at 7162.94 and 7162.989 cm^{-1}, respectively, have been found incorrect.

4. Line intensities and comparison with databases

For proper comparison, we excluded from our set of 2015 $H_2{}^{18}O$ lines, all the lines superimposed with transitions of other isotopologues and some of the lines observed as a weak shoulder of much stronger line, leaving 1790 line strengths for comparison.

Table 3
New experimental energy levels of the $HD^{18}O$ molecule (in cm^{-1}) derived by CW-CRDS in the 5905.7–6725.7 cm^{-1}.

$V_1V_2V_3$	J	K_a	K_c	E_{obs}	δE	N	Δ	$V_1V_2V_3$	J	K_a	K_c	E_{obs}	δE	N	Δ
021	2	0	2	6471.7423	1.4	4	0.02	101	8	6	3	7438.3973	1.4	3	0.05
021	5	1	5	6649.1608*	0.3	3	0.02	101	8	6	2	7438.3968	1.4	4	0.05
021	6	1	6	6729.7163	0.1	3	0.02	101	9	1	8	7104.1771	1.3	6	0.05
021	6	2	4	6840.0066	0.4	4	0.04	101	9	3	7	7203.4834	0.5	6	0.04
021	6	6	1	7377.4143	0.4	3	0.09	101	9	3	6	7223.8082	0.8	3	0.04
021	6	6	0	7377.4143	0.4	3	0.09	101	9	4	6	7303.6422	0.5	4	0.05
021	7	2	5	6957.6130*	0.7	2	0.02	101	9	4	5	7306.3285	1.1	3	0.04
021	7	3	4	7029.6866*	1.2	4	0.04	101	9	5	5	7425.7234	1.0	3	0.04
021	7	5	3	7301.1603	1.3	3	0.07	101	9	5	4	7425.8673	0.5	3	0.04
021	7	5	2	7301.1674	0.1	2	0.07	101	9	6	4	7573.8194		1	0.05
021	7	6	2	7485.4553	0.1	2	0.08	101	9	6	3	7573.8236	0.6	2	0.05
021	7	6	1	7485.4553	0.0	2	0.08	101	10	1	9	7248.0503	1.4	5	0.04
021	7	7	1	7697.6928		1	0.11	101	10	2	9	7251.3484	0.4	4	0.04
021	7	7	0	7697.6928		1	0.11	101	10	2	8	7328.2308	0.8	2	0.04
021	8	2	7	7041.3287*	0.3	3	0.03	101	10	3	8	7353.1780	0.1	4	0.04
021	8	2	6	7091.4591		1	0.02	101	10	3	7	7385.0280	1.3	3	0.04
021	8	4	5	7271.9949	1.4	3	0.05	101	10	4	7	7455.9729	0.7	3	0.04
021	8	4	4	7272.9669	0.3	3	0.05	101	10	4	6	7461.6728	0.8	2	0.04
021	8	5	4	7425.4054		1	0.07	101	10	5	6	7577.4644	0.9	3	0.03
021	8	5	3	7425.4402		1	0.07	101	10	5	5	7577.8316	0.8	2	0.04
021	8	6	3	7608.9992		1	0.08	101	10	6	4	7724.4631		1	0.04
021	8	6	2	7609.0015	0.6	2	0.08	101	11	1	10	7403.5720	0.4	4	0.04
021	9	0	9	7046.0458	0.1	2	0.02	101	11	2	10	7405.4208	0.6	2	0.04
021	9	1	9	7046.4736	1.2	4	0.02	101	11	2	9	7498.9875	1.1	3	0.04
021	9	1	8	7164.1463*	0.5	3	0.02	101	11	3	9	7516.5718		1	0.04
021	9	2	8	7172.8880		1	0.03	101	11	3	8	7562.5209		1	0.04
021	9	2	7	7240.8550	0.5	2	0.02	101	11	4	8	7623.2590		1	0.03
021	9	3	7	7287.0648	0.1	2	0.03	101	11	4	7	7634.1926		1	0.04
021	9	3	6	7308.3042	0.2	2	0.03	101	11	5	7	7744.3680		1	0.03
021	9	4	6	7412.7441	1.4	2	0.04	101	11	5	6	7745.5512		1	0.03
021	9	4	5	7415.1355		1	0.05	101	12	0	12	7428.7867	1.2	2	0.04
021	9	5	5	7565.3475	0.4	2	0.06	101	12	1	12	7428.8193		1	0.04
021	9	5	4	7565.4653	0.7	2	0.06	101	12	1	11	7570.8393	0.9	2	0.03
021	10	1	10	7176.6856	0.8	3	0.02	101	12	2	11	7571.8480	0.8	2	0.03
021	10	1	9	7312.0006	0.5	2	0.03	101	12	2	10	7681.6015		1	0.03
021	10	2	9	7317.4100	0.6	2	0.03	101	12	3	10	7693.2490		1	0.03
021	10	3	8	7441.2152	0.1	2	0.04	101	12	3	9	7755.3353		1	0.03
021	10	3	7	7474.3920		1	0.03	101	12	4	8	7824.1478		1	0.03

021	10	5	5	7721.3146	0.7	2	0.06	101	12	5	8	7926.7286		1	0.01
021	11	0	11	7318.9724	0.3	2	0.02	101	13	0	13	7594.8010		1	0.04
021	11	1	11	7319.0877	0.4	3	0.02	101	13	1	13	7594.8162		1	0.04
021	11	1	10	7471.3976		1	0.03	101	13	1	12	7749.9558		1	0.03
021	11	2	10	7474.6118		1	0.03	101	13	2	12	7750.4894	1.5	2	0.03
021	11	2	9	7582.0173		1	0.03	101	13	3	11	7882.8196		1	0.02
021	11	3	8	7657.6657		1	0.03	101	13	4	9	8031.4220		1	0.02
021	11	5	7	7892.4227		1	0.04	101	13	5	9	8124.2966		1	0.02
021	12	0	12	7473.5796		1	0.02	101	14	0	14	7772.8831		1	0.02
021	12	1	12	7473.6412		1	0.03	101	14	1	14	7772.8921	0.6	2	0.02
021	12	2	11	7644.2666		1	0.03	101	14	1	13	7940.9789		1	0.02
021	12	2	10	7771.7527		1	0.03	101	14	2	13	7941.2500		1	0.02
101	7	5	3	7168.3983*	0.1	3	0.06	101	15	0	15	7963.0308		1	0.03
101	7	5	2	7168.4069*	0.5	3	0.05	101	15	1	15	7963.0283		1	0.02
101	7	7	1	7493.1319		1	0.07	210	3	3	1	6951.8100**		1	0.03
101	7	7	0	7493.1319		1	0.07	210	3	3	0	6951.8347**	0.2	2	0.03
101	8	3	6	7067.8963	1.2	5	0.05	210	5	2	3	7008.5366		1	0.07
101	8	3	5	7079.5830	0.4	5	0.05	210	5	4	1	7202.3199		1	0.01
101	8	4	5	7166.6285	1.2	4	0.05	210	6	4	2	7292.2348		1	0.03
101	8	4	4	7167.6766	0.6	4	0.05	210	7	1	6	7161.9427		1	0.09
101	8	5	4	7289.3962	0.7	3	0.05	210	7	2	5	7217.4913	1.9	2	0.08
101	8	5	3	7289.4389	1.1	4	0.05	210	7	3	4	7286.7942		1	0.06
210	7	4	3	7397.4122		1	0.02	210	9	4	5	7654.5831		1	0.04
210	8	0	8	7204.1129*		1	0.06	210	10	1	9	7564.5538		1	0.09
210	8	1	8	7205.7866		1	0.06	210	10	2	9	7571.0732		1	0.08
210	8	1	7	7285.5954		1	0.09	210	10	2	8	7648.1163		1	0.06
210	8	2	7	7302.4475		1	0.07	210	10	3	8	7684.8093		1	0.06
210	8	2	6	7346.1842		1	0.09	210	11	1	10	7720.3565		1	0.08
210	8	3	6	7401.9325*		1	0.05	210	11	3	9	7847.1188		1	0.08
210	8	3	5	7411.5175		1	0.06	050	4	1	3	6866.2473		1	0.09
210	9	0	9	7321.0560		1	0.06	050	5	1	5	6898.3241		1	0.08
210	9	1	9	7322.2192		1	0.06	050	7	1	7	7071.2691		1	0.09
210	9	2	8	7430.3954		1	0.08	050	8	1	8	7176.4536		1	0.09
210	9	2	7	7489.9647		1	0.01	050	9	0	9	7290.5977		1	0.09
210	9	3	7	7536.2981		1	0.06								

Notes: N is the number of lines used for the upper level determination. δE (in $10^{-3}\,cm^{-1}$) denotes the corresponding statistical error defined as the *rms* value of the deviation of the levels derived through several transitions. Δ represents the deviation of the experimental levels from their calculated values [24] in cm^{-1}. The energies of the levels marked by * were previously derived [24] with a different value (absolute deviations between 0.012 and $0.025\,cm^{-1}$). The levels [3 3 1], [3 3 0] of the (210) state marked by ** are incorrect in the dataset of Ref. [25].

Table 4
New experimental energy levels of the $H_2{}^{17}O$ molecule (in cm^{-1}) derived by CW-CRDS in the 5905.7–6725.7 cm^{-1} region.

$V_1V_2V_3$	J	K_a	K_c	E_{obs}	N	Δ	$V_1V_2V_3$	J	K_a	K_c	E_{obs}	δE	N	Δ
011	8	8	1	7163.0460	1	0.00	040	5	2	3	6650.2173	0.5	2	−0.02
011	8	8	0	7163.0512	1	0.00	040	5	3	3	6806.9351		1	−0.02
011	9	9	1	7605.9654	1	0.01	040	5	3	2	6808.5281		1	−0.02
011	9	9	0	7605.9659	1	0.01	040	5	4	1	7024.1675		1	−0.01
011	10	7	4	7415.6784	1	−0.03	040	5	5	1	7275.5855		1	−0.01
011	10	7	3	7415.7040	1	−0.03	040	5	5	0	7275.5851		1	−0.02
011	10	9	1	7850.2933	1	−0.01	040	6	2	5	6766.9033		1	−0.02
011	11	8	4	7891.0520	1	−0.03	040	7	1	7	6721.1063		1	0.00
011	12	3	9	7429.2794	1	−0.02	040	9	0	9	7046.9265		1	0.00
011	12	5	8	7610.4285	1	−0.06	120	4	4	0	7339.8683		1	0.00
011	12	7	5	7969.4837	1	−0.06	120	6	6	0	7980.7356		1	−0.03
011	13	3	11	7560.2330	1	−0.03	120	7	3	5	7625.8721		1	−0.01
040	1	0	1	6145.2637	1	0.00	120	8	4	4	7970.5549		1	−0.01
040	1	1	0	6188.1500	1	−0.01	120	8	5	4	8139.7585		1	−0.02
040	3	1	3	6284.4009	1	−0.01	120	9	1	9	7661.6753		1	0.04
040	3	2	1	6420.0747	1	−0.01	120	10	1	9	8065.1636		1	0.00
040	4	0	4	6347.6909	1	−0.01	120	10	3	8	8240.1615		1	−0.02
040	4	3	1	6686.0600	1	−0.01	120	11	0	11	8053.6761		1	0.04
040	5	1	5	6465.4183	1	0.00	120	11	1	11	8054.6667		1	0.03

Notes: N is the number of lines used for the upper level determination. δE (in 10^{-3} cm^{-1}) denotes the corresponding statistical error defined as the *rms* value of the deviation of the levels derived through several transitions. Δ represents the deviation of the experimental levels from their calculated [9] values in cm^{-1}.

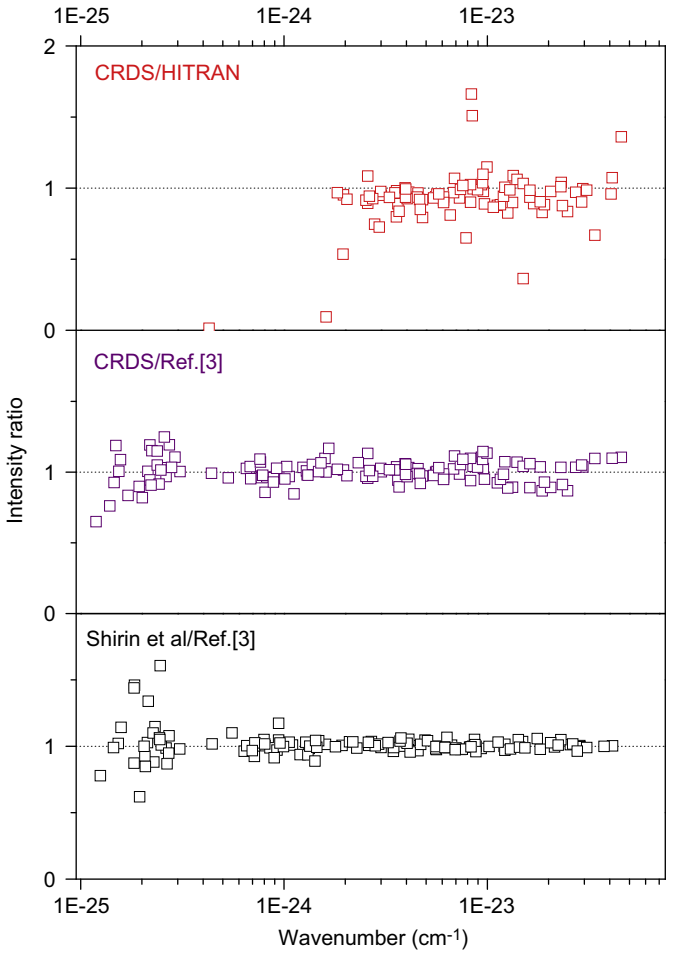

Fig. 7. Comparison of the intensity values of $H_2{}^{18}O$ transitions measured in the 5905–6725 cm^{-1} region. *Upper panel:* ratio of CW-CRDS to HITRAN values. *Middle panel*: ratio of CW-CRDS values to the values obtained by FTS by Chevillard et al. [3]. *Lower panel*: ratio of the values obtained by Chevillard et al. [3] and Shirin et al. variational calculations [9].

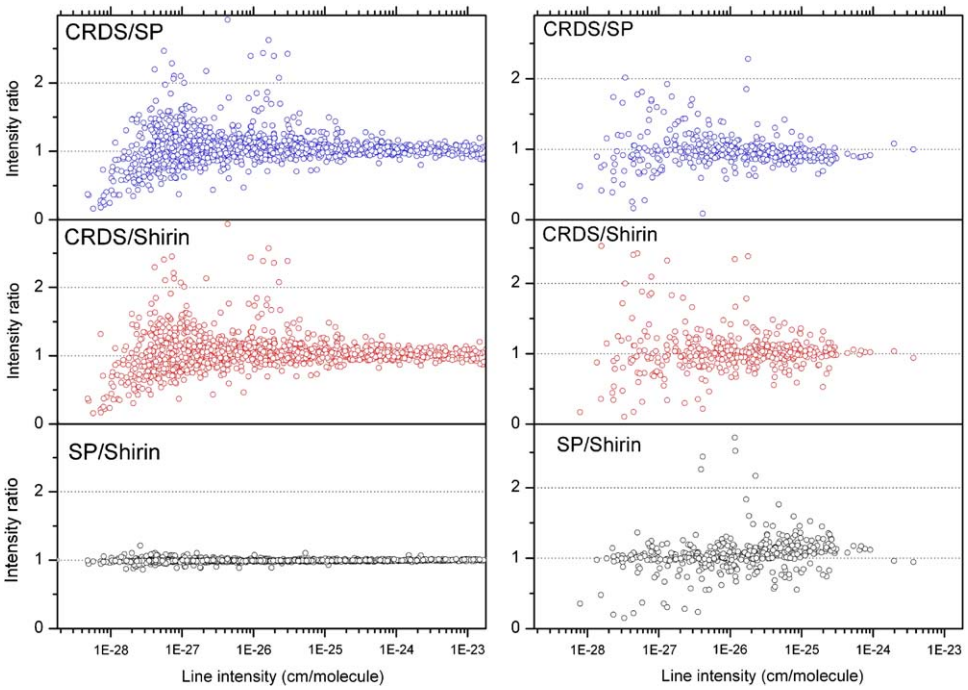

Fig. 8. Ratios of the experimental intensity values by the calculated values obtained by Schwenke and Partridge [10] and Shirin et al. [9] for the $H_2{}^{18}O$ transitions recorded by CW-CRDS between 5905 and 6725 cm^{-1}. The left hand panels are relative to all the transitions measured by CW-CRDS except those of the $4v_2$ band, the right hand panel is relative to the $4v_2$ band. (see text.)

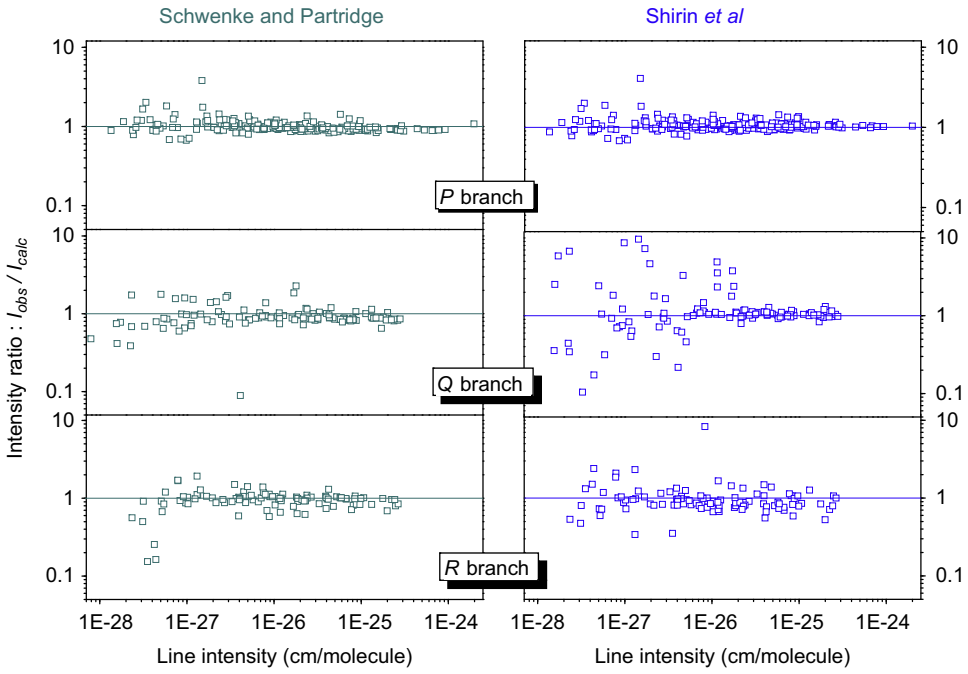

Fig. 9. Branch by branch comparison of the experimental intensity values to the calculated values obtained by Schwenke and Partridge [10] and Shirin et al. [9] for the $4v_2$ band of $H_2{}^{18}O$. Note the logarithmic scale adopted for the ordinate axis.

4.1. Comparison with previous experimental data

The intensity measurements for $H_2{}^{18}O$ in the spectral region under study are available from spectra of water in natural abundance [7,8,14] and from spectra of ^{18}O enriched water [3,4]. As the uncertainties on the intensity values are expected

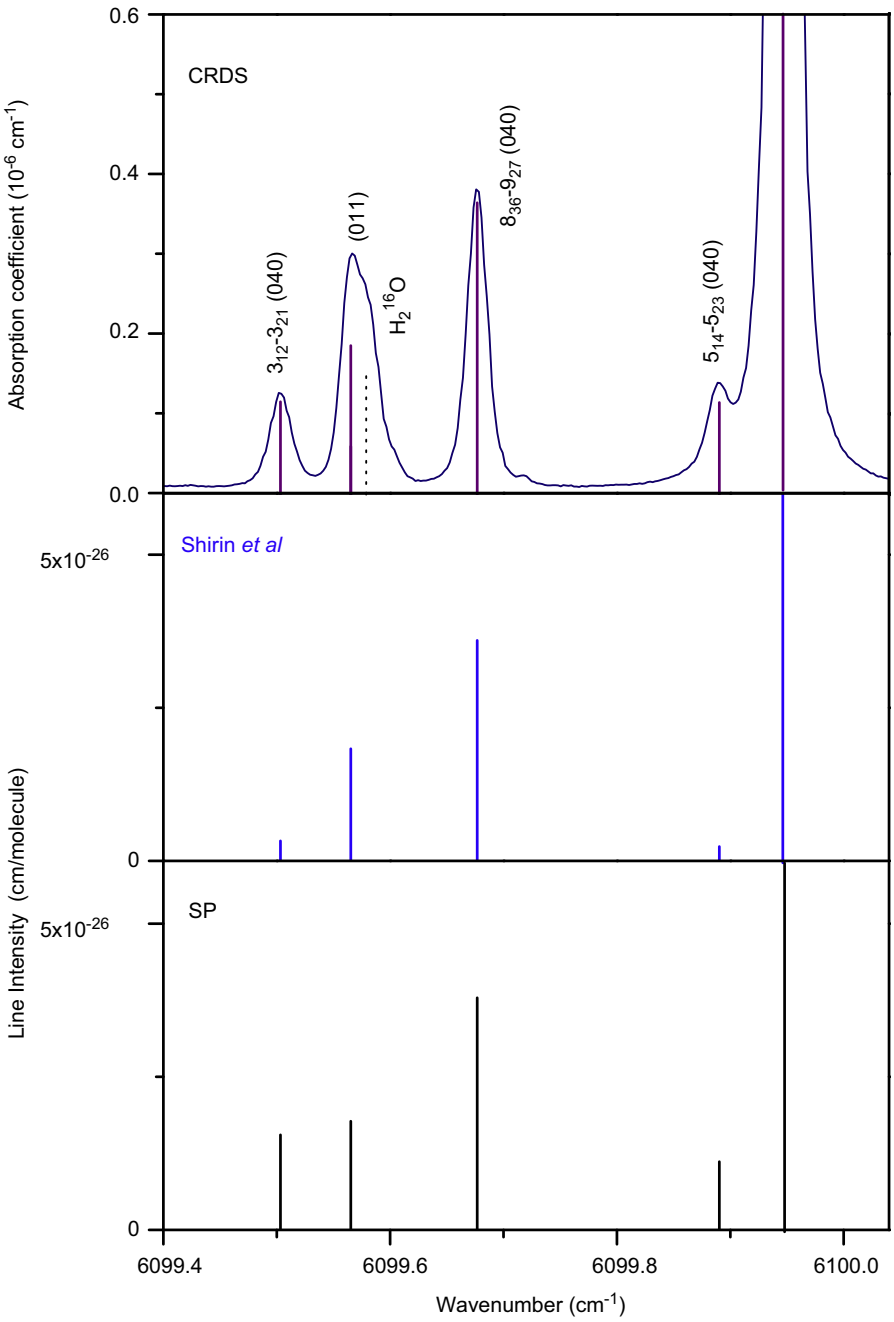

Fig. 10. An example of disagreement between the measured and variationally computed intensities of $4\nu_2$ transitions of $H_2{}^{18}O$. For an easier comparison, the calculated line positions have been adjusted to their experimental values. *Upper panel*: CW-CRDS spectrum. The superimposed stick spectrum corresponds to the $H_2{}^{18}O$ CRDS line list. The assignment of three $4\nu_2$ transitions of interest is indicated. *Middle panel*: calculated spectrum obtained by Shirin et al. [9]. *Lower panel*: calculated spectrum obtained by Schwenke and Partridge [10].

to be larger for measurements performed with natural water, we will discuss mainly the results obtained with ^{18}O enriched samples. Only rough intensity values were reported from Hefei spectra [5,6]. The comparison is then limited to about a hundred of strong lines (intensity values larger than 10^{-25} cm/molecule) reported by Chevillard et al. [3], and Toth's results [4,27] which were adopted in the HITRAN database for $H_2{}^{18}O$ in our region. On average, HITRAN values (90 lines) are overestimated by 6% compared to our values while a perfect coincidence is noted with Ref. [3] (126 lines, average intensity ratio of 1.00). Note that intensities values of Ref. [3] were preliminary transformed from 300 to 296 K for comparison.

Table 5
Comparison of the measured intensities of some transitions of the $4\nu_2$ band of $H_2{}^{18}O$ to the calculated values obtained by Schwenke and Partridge [10] and Shirin et al. [9]. The selected transitions show important discrepancies between the two calculations (see Text).

Wavenumber (cm^{-1})	Intensity (cm/molecule)	J K_a K_c						I_{obs}/I_{calc}		Branch	ΔK_a	ΔK_c
	Obs.	Up			Low			SP [10]	Ref. [9]			
6054.956	2.30E−27	4	1	4	4	2	3	1.06	0.29	Q	−1	1
6061.453	1.12E−27	4	0	4	4	1	3	0.75	1037.45	Q	−1	1
6071.747	1.55E−28	10	2	9	10	3	8	0.74	0.35	Q	−1	1
6075.818	1.73E−26	3	0	3	3	1	2	0.83	3.77	Q	−1	1
6085.924	1.16E−26	2	0	2	2	1	1	0.86	2.34	Q	−1	1
6089.390	5.36E−28	7	1	6	7	2	5	0.64	83.12	Q	−1	1
6092.099	4.11E−27	1	0	1	1	1	0	0.08	0.21	Q	−1	1
6095.580	1.71E−27	2	1	1	2	2	0	0.83	7.28	Q	−1	1
6095.836	1.44E−27	6	1	5	6	2	4	0.98	9.64	Q	−1	1
6099.503	1.16E−26	3	1	2	3	2	1	0.74	3.55	Q	−1	1
6099.890	1.15E−26	5	1	4	5	2	3	1.02	4.91	Q	−1	1
6100.811	2.32E−28	7	2	6	7	3	5	1.74	0.34	Q	−1	1
6101.138	4.68E−27	4	1	3	4	2	2	0.75	3.29	Q	−1	1
6108.510	4.44E−28	6	2	5	6	3	4	0.78	0.17	Q	−1	1
6119.018	3.28E−28	4	2	3	4	3	2	0.68	0.10	Q	−1	1
6135.432	9.88E−28	6	2	4	6	3	3	0.97	8.65	Q	−1	1
6136.752	2.32E−28	9	2	7	9	3	6	0.68	6.75	Q	−1	1
6137.485	1.95E−27	7	2	5	7	3	4	0.78	4.65	Q	−1	1
6137.802	1.58E−28	8	2	6	8	3	5	0.41	2.52	Q	−1	1
6143.965	1.31E−27	2	0	2	1	1	1	1.11	0.34	R	−1	1
6187.736	8.31E−27	2	1	2	1	0	1	0.69	8.30	R	1	1
6188.891	5.89E−28	4	3	2	4	4	1	0.85	0.31	Q	−1	1
6192.622	1.73E−28	9	3	6	9	4	5	0.77	5.85	Q	−1	1
6202.811	3.53E−27	3	1	3	2	0	2	1.50	0.35	R	1	1
6274.252	7.91E−29	6	4	3	6	5	2	0.47	0.16	Q	−1	1
6325.426	3.53E−28	4	2	3	3	1	2	0.15	1.31	R	1	1
6413.795	4.40E−28	5	2	3	4	1	4	0.16	2.40	R	1	−1
6528.301	4.23E−28	6	3	3	5	2	4	0.25	1.50	R	1	−1

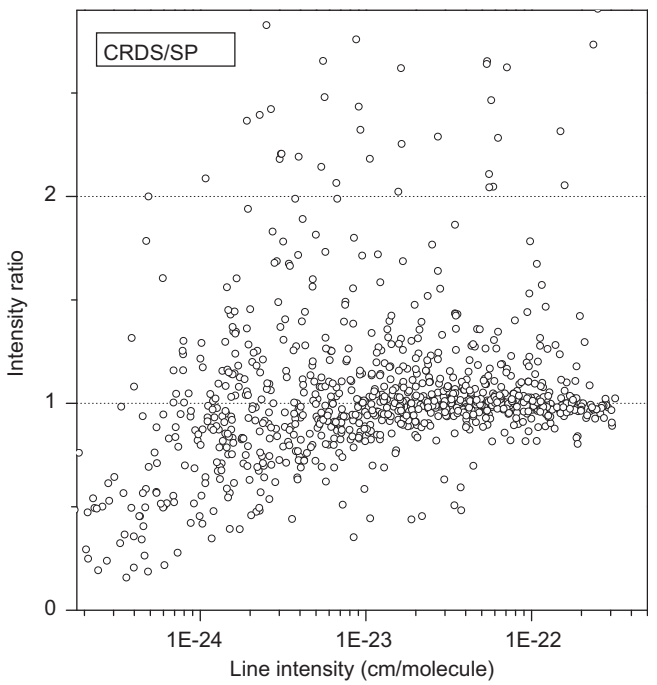

Fig. 11. Ratio of the experimental intensity values by the calculated values [10,24] versus the experimental line intensity for $HD^{18}O$ transitions recorded by CW-CRDS between 5905 and 6725 cm^{-1}. The intensity values are relative to the pure species.

The values of Ref. [3] shows a better agreement to the variationally calculated intensities [9] (lower panel of Fig. 7) than to our values (middle panel). This probably indicates that the uncertainty on CW-CRDS intensities is on the order of 5% for the strongest lines as a consequence of the low pressures used for the recordings above 6600 cm^{-1}.

Finally, compared to our preceding $H_2{}^{18}O$ intensities values obtained in Ref. [7], the overall agreement is satisfactory, considering the weakness of the line intensities measured with water in natural abundance. We nevertheless noted a 10% systematic underestimation of the intensities of the strongest intensities compared to the present measurements. We could not perform reasonable comparison with the 137 $H_2{}^{18}O$ lines in common with Ref. [14] as these lines were among the weakest in Ref. [14] and their intensities are reported with large uncertainties.

4.2. Comparison with variational calculations

The agreement between the experimental intensities and variational calculations [9,10] was one of the main criteria used in the assignment process. On Fig. 8, the ratios of the CW-CRDS and variational [9,10] intensities are presented separately for the $4v_2$ transitions and for all other transitions. The particular case of the $4v_2$ transitions is discussed in the next subsection. For all transitions different from those of the $4v_2$ band, a very good agreement is noted over a 5 decades dynamic of the measured intensities (2×10^{-28}–3×10^{-23} cm/molecule). The average I_{obs}/I_{calc} ratio is 1.045 both for SP and Shirin et al. calculations. We have also directly compared Shirin et al. calculations based on a new dipole moment surface [28] to SP intensity values. The agreement between the two calculations is much better than with the experimental values but this result does not apply to the transitions of the $4v_2$ band.

4.3. The $4v_2$ band

Indeed, important disagreements between the two calculations appear for the $4v_2$ band transitions. A line by line examination of the two calculations shows that the largest (up to three orders of magnitude) discrepancies concern transitions of the *Q* and *R* branches. Fig. 9 shows the ratios of the CRDS intensities to the predicted values for the *P*, *Q* and *R* branches of the $4v_2$ band both for SP [10] and Shirin et al. [9]. None of the two calculations reproduce satisfactorily the observations. On one hand, experimental intensities of the strongest lines are systematically weaker by about 10–12% compared to SP calculations and agree better with Ref. [9]. This is confirmed by the ratio of the total experimental and calculated intensities of the $4v_2$ transitions which is 0.93 and 0.99 for SP and Shirin et al., respectively. On the other hand, the I_{obs}/I_{calc} ratios of the weak lines ($<10^{-26}$ cm/molecule) show a higher dispersion for Shirin et al., in particular in the *Q* and *R* branches. For instance, the intensity of the [404]–[413] transition at 6061.453 cm^{-1} (1.12×10^{-27} cm/molecule) which is largely above the sensitivity threshold, is calculated [9] more than three orders of magnitude weaker than observed while SP intensity value falls in good coincidence (1.49×10^{-27} cm/molecule). Another example is illustrated by the spectrum near 6100 cm^{-1} displayed in Fig. 10. The situation is better but not yet satisfactory for the *R*-branch: I_{obs}/I_{calc} ratios range from 0.34 to 8.3. The largest discrepancies between the calculations and the experimental values are included in Table 5. Interestingly, most of the largest errors in Shirin et al. calculations concern $\Delta K_a=-1$, $\Delta K_c=1$ transitions of the *Q* branch. Another finding is that the differences between intensities provided by the two calculations [9,10] are less pronounced for transitions with K_a values higher than 3 and for transitions with $|K_a-K_c|>1$. Of course, for the weakest transitions, intensity comparison with the calculated databases is limited by the increasing uncertainty on the measured values but the evidenced deviations largely exceed the experimental uncertainty for most of the lines.

Despite the fact that Shirin et al. intensities are probably more accurate for the strongest lines of the $4v_2$ band, the SP database is largely preferable for the assignment of the $4v_2$ band as it does not present sudden variations of the intensities ratios over all the range of the experimental intensity values (1.0×10^{-28}–1.0×10^{-24} cm/molecule). The complete comparison of the $4v_2$ transition intensities with Shirin et al. and SP data is included in the Supplementary material.

As it could be anticipated, a detailed analysis of the $H_2{}^{16}O$ intensity values measured in this study and in Refs. [7,14,29] revealed similar large intensity discrepancies between Refs. [9,10] for the $4v_2$ band of the main isotopologue.

4.4. $HD^{18}O$ isotopologue

The measured $HD^{18}O$ line intensities have been compared (Fig. 11) with those calculated by Tashkun [24] using the potential energy and dipole moment surfaces given by Partridge and Schwenke [10] and a higher dimension basis. As the relative abundance of $HD^{18}O$ in our sample was unknown, the calculated absolute intensities were scaled in order to match on average the observed values. It yielded a factor of 2.79×10^{-4} for the $HD^{18}O$ abundance relative to the $H_2{}^{18}O$ species which is close to the natural $HD^{18}O/H_2{}^{18}O$ abundance (3.11×10^{-4}). In our spectral region, previous intensity measurements of $HD^{18}O$ transitions were limited to 320 lines observed recently in FTS spectra recorded with natural ^{18}O abundance [25]. Our intensity values agree better with the variational calculations than with the results of Ref. [25], probably indicating that larger errors affect these measurements.

5. Conclusion

The experimental knowledge of $H_2{}^{18}O$ absorption spectrum near 1.6 μm has been significantly improved by CW-CRDS. The high linearity and high dynamics of our CW-CRDS spectrometer have allowed measuring intensities ranging between 10^{-28} and 10^{-23} cm/molecule. For comparison, the weakest transitions previously detected in the region have intensities on the order of 10^{-26} cm/molecule (Fig. 4) while the HITRAN intensity cut-off is 1.7×10^{-24} cm/molecule.

1976 of the 2804 $H_2{}^{18}O$ and $HD^{18}O$ lines measured between 5905.7 and 6725.7 cm^{-1} are reported for the first time. The $H_2{}^{18}O$ transitions belong to a total of 18 bands whose upper state vibrational energies range between 4648 and 9795 cm^{-1}. 288, 135 and 38 new energy levels were derived for the $H_2{}^{18}O$, $HD^{18}O$ and $H_2{}^{17}O$ isotopologues, respectively. They include the vibrational origin of the $4\nu_2$ band at 6110.4238 cm^{-1} and 24 energy levels of the (050) bending state together with levels with J and K_a values as large as 18 and 12 for the strong $\nu_2+\nu_3$ band.

An estimation of the average accuracy of our energy values can be obtained from the *rms* values of the deviations of the 600 levels of $H_2{}^{18}O$, $HD^{18}O$ and $H_2{}^{17}O$ derived through several transitions. We obtain a value of 4.7×10^{-4} cm^{-1} and then believe that our energy levels values are in general preferable when they differ significantly from the energy values of Ref. [11] ($H_2{}^{18}O$ and $H_2{}^{17}O$) or Ref. [25] ($HD^{18}O$). This is particular the case of the $HD^{18}O$ species for which, in addition to the 135 new energy levels, the overall accuracy of 171 energy levels previously reported in Ref. [25] could be improved from the extensive use of combination differences relations allowed by the increased sensitivity of our recordings.

Transitions reported in this study for the $H_2{}^{16}O$ and $HD^{16}O$ isotopologues are found to be in a good agreement with previous experimental data. Even if new assignments were not obtained for these two isotopologues, they are given in the line list attached as Supplementary Material as they may be included in the MARVEL code in order to derive a consistent set of rovibrational energy levels.

In the assignment process, the list of $H_2{}^{18}O$ and $H_2{}^{17}O$ energy levels recently validated by the IUPAC TG [11] was found useful to help for the assignment of transitions reaching known energy levels and for an exhaustive comparison with previous investigations. The newly determined energy levels are upper levels of not yet observed transitions whose line positions can be now accurately calculated. By this way, the MARVEL procedure will help to propagate the impact of the reported new observations in nearby spectral regions. This advantage, which is a simple consequence of the Ritz principle, will be particularly marked in the present case as a number of new energy levels could be derived from hot bands transitions reaching upper vibrational states located far above the investigated spectral region (up to 9795 cm^{-1}).

The variationally computed and the measured intensities were found in very good agreement over the five decades dynamics of intensities values. This is true for all the bands except the $4\nu_2$ band for which some of the measured intensity values deviate importantly from the variational results obtained by both Schwenke and Partridge [10] and Shirin et al. [9]. These disagreements are particularly marked for some weak lines calculated by Shirin et al. and concern mostly, the Q-branch transitions with small K_a values. We checked that the (040) state can be treated as an isolated state for the involved upper energy levels and concluded that the evidenced perturbations cannot be explained by resonance perturbations of the corresponding rovibrational functions. Calculations of the $4\nu_2$ band transitions intensities with the same DMS [28] and different PES are needed to confirm that the inaccuracies of the resulting DMS [28] are responsible for the encountered disagreement with the experiment. Note that similar deviations between measured and computed intensities exist for the $H_2{}^{16}O$ main isotopologue. It indicates that while variationally computed intensities are close (better?) to the experimental accuracy for most of the bands, in the case of the pure bending overtones, measured intensities values may be preferred when available.

Acknowledgements

This work was performed as part of the IUPAC task group (no 2004-035-1-100) to "compile, determine, and validate, both experimentally and theoretically, a database of water transitions". It is jointly supported by CNRS (France), RFBR (Russia) and CAS (China) in the frame of Groupement de Recherche International SAMIA (Spectroscopy of Molecules of Atmospheric Interest). The support of the Programme National LEFE (CHAT) INSU-CNRS is acknowledged, as well as that of grant no. 06-03-39014 RFBR (Russia)–NNSF (China). ON is grateful to Grenoble University for a visiting professorship during February–April, 2009. We are indebted to SN Mikhailenko (Tomsk, Russia) for communicating unpublished data and to AG Császár (Budapest, Hungary) for a careful reading of the manuscript and valuable suggestions.

Appendix A. Supplementary material

Supplementary data associated with this article can be found in the online version at doi:10.1016/j.jqsrt.2009.04.013.

References

[1] Rothman LS, Jacquemart D, Barbe A, Benner DC, Birk M, Brown LR, et al. The HITRAN 2004 molecular spectroscopy database. JQSRT 2005;96:139–204.
[2] Rothman LS, Gordon IE, Barbe A, Benner DC, Bernath PF, Birk M, et al. The HITRAN 2008 molecular spectroscopic database. JQSRT 2009;110:533–72.

[3] Chevillard JP, Mandin JY, Flaud JM, Camy-Peyret C. The first hexad [(040), (120), (021), (200), (101), (002)] of $H_2^{18}O$: experimental energy levels and line intensities. Can J Phys 1986;64:746–61.
[4] Toth RA. Transition frequencies and strengths of $H_2^{17}O$ and $H_2^{18}O$: 6600–7640 cm^{-1}. Appl Opt 1994;33:4868–79.
[5] Liu AW, Du JH, Song KF, Wang L, Wan L, Hu SM. High-resolution Fourier-transform spectroscopy of ^{18}O enriched water molecule in the 1080–7800 cm^{-1} region. J Mol Spectrosc 2006;237:149–62.
[6] Liu AW, Naumenko O, Song KF, Voronin BA, Hu SM. Fourier transform absorption spectroscopy of $H_2^{18}O$ in the first hexade region. J Mol Spectrosc 2006;236:127–33.
[7] Macko P, Romanini D, Mikhailenko SN, Naumenko OV, Kassi S, Jenouvrier A, et al. High sensitivity CW-cavity ring down spectroscopy of water in the region of the 1.5 μm atmospheric window. J Mol Spectrosc 2004;227:90–108.
[8] Mikhailenko SN, Wang L, Kassi S, Campargue A. Weak water absorption lines around 1.455 and 1.66 μm by CW-CRDS. J Mol Spectrosc 2007;244:170–8.
[9] Shirin SV, Polyansky OL, Zobov NF, Ovsyannikov RI, Csaszar AG, Tennyson J. Spectroscopically determined potential energy surfaces of the $H_2^{16}O$, $H_2^{17}O$, and $H_2^{18}O$ isotopologues of water. J Mol Spectrosc 2006;236:216–23.
[10] Schwenke DW, Partridge H. Convergence testing of the analytic representation of an ab initio dipole moment function for water: improved fitting yields improved intensities. J Chem Phys 2000;113:6592–7.
[11] Tennyson J, Bernath PF, Brown LR, Campargue A, Carleer MR, Császár AG, et al. IUPAC critical evaluation of the rotational–vibrational spectra of water vapor. Part I. Energy levels and transition wavenumbers for $H_2^{17}O$ and $H_2^{18}O$. JQSRT 2009;110:573–96.
[12] Furtenbacher T, Császár AG, Tennyson J. MARVEL: measured active rotational–vibrational energy levels. J Mol Spectrosc 2007;245:115–25.
[13] Furtenbacher T, Császár AG. On employing $H_2^{16}O$, $H_2^{17}O$, $H_2^{18}O$, and $D_2^{16}O$ lines as frequency standards in the 15–170 cm^{-1} window. JQSRT 2008;109:1234–51.
[14] Jenouvrier A, Daumont L, Régalia-Jarlot L, Tyuterev VG, Carleer M, Vandaele AC, et al. Fourier transform measurements of water vapor line parameters in the 4200–6600 cm^{-1} region. JQSRT 2007;105:326–55.
[15] Chevillard JP, Mandin JY, Flaud JM, Camy-Peyret C. $H_2^{18}O$: The (030), (110), and (011) interacting states. Line positions and intensities $3\nu_2$, $\nu_1+\nu_2$, and $\nu_2+\nu_3$ bands. Can J Phys 1985;63:1112–27.
[16] Perevalov BV, Kassi S, Perevalov VI, Tashkun SA, Campargue A. High sensitivity CW-CRDS spectroscopy of $^{12}C1^6O_2$, $^{16}O^{12}C^{17}O$ and $^{16}O^{12}C^{18}O$ between 5851 and 7045 cm^{-1}: line positions analysis and critical review of the current databases. J Mol Spectrosc 2008;252:143–59.
[17] Perevalov BV, Campargue A, Gao B, Kassi S, Tashkun SA, Perevalov VI. New CW-CRDS measurements and global modeling of $^{12}C^{16}O_2$ absolute line intensities in the 1.6 μm region. J Mol Spectrosc 2008;252:190–7.
[18] Perevalov BV, Perevalov VI, Campargue A. A (nearly) complete experimental linelist for $^{13}C^{16}O_2$, $^{16}O^{13}C^{18}O$, $^{16}O\ ^{13}C^{17}O$, $^{13}C_2^{18}O$ and $^{17}O\ ^{13}C^{18}O$ by high sensitivity CW-CRDS spectroscopy between 5851 and 7045 cm^{-1}. JQSRT 2008;109:2437–62.
[19] Liu AW, Kassi S, Perevalov VI, Hu SM, Campargue A. High sensitivity CW-cavity ring down spectroscopy of N_2O near 1.5 μm (III). J Mol Spectrosc 2009;254:20–7.
[20] Campargue A, Barbe A, De Backer-Barilly MR, Tyuterev VI G, Kassi S. The near infrared spectrum of ozone by CW-cavity ring down spectroscopy between 5850 and 7000 cm^{-1}: new observations and exhaustive review. Phys Chem Chem Phys 2008;10:2925–46.
[21] Morville J, Romanini D, Kachanov AA, Chenevier M. Two schemes for trace detection using cavity ringdown spectroscopy. Appl Phys 2004;D78:465–76.
[22] Perevalov BV, Kassi S, Romanini D, Perevalov VI, Tashkun SA, Campargue A. CW-cavity ringdown spectroscopy of carbon dioxide isotopologues near 1.5 μm. J Mol Spectrosc 2006;238:241–55.
[23] Partridge H, Schwenke DW. The determination of an accurate isotope dependent potential energy surface for water from extensive ab initio calculations and experimental data. J Chem Phys 1997;106:4618–39.
[24] 〈http://spectra.iao.ru〉.
[25] Mikhailenko SN, et al. Critical evaluation of measured rotation–vibration transitions and an experimental dataset of energy levels of $HD^{18}O$. JQSRT 2009; doi:10.1016/j.jqsrt.2009.01.012.
[26] Mikhailenko SN, Tyuterev VG, Mellau G. (000) and (010) states of $H_2^{18}O$: analysis of rotational transitions in hot emission spectrum in the 400–850 cm^{-1} region. J Mol Spectrosc 2003;217:195–211.
[27] Toth RA, 〈http://www.mark4sun.jpl.nasa.gov〉.
[28] Lodi L, Tolchenov RN, Tennyson J, Lynas-Gray AE, Shirin SV, Zobov NF, et al. A new ab initio ground-state dipole moment surface for the water molecule. J Chem Phys 2008;128:044304.
[29] Mikhailenko SN, Keppler Albert KA, Mellau G, Klee S, Winnewisser BP, Winnewisser M, et al. Water vapour absorption line intensities in the 1900–6600 cm^{-1} region. JQSRT 2008;109:2687–96.